AUGMENTATION OF HEAT TRANSFER DURING POOL BOILING OF REFRIGERANT

A DISSERTATION

Submitted in partial fulfillment of the requirements

for the award of the degree

Of

MASTER OF TECHNOLOGY

In

THERMAL ENGINEERING

By

SUDHIR KUMAR VERMA

Department of Mechanical and Industrial Engineering

Indian Institute of Technology Roorkee

Roorkee-247667 (INDIA)

MAY, 2018

Candidate's Declaration

I hereby declare that the work carried out in this dissertation titled, **"Augmentation of Heat Transfer During Pool Boiling of Refrigerant"**, is presented on behalf of partial fulfillment of the requirement for the award of degree of **"Master of Technology"** in Mechanical and Industrial Engineering Department with specialization **Thermal Engineering** of Indian Institute of Technology Roorkee, Roorkee, India, is an authentic record of my own work carried out under the supervision of Dr. Anil Kumar, Associate Professor, MIED, IIT Roorkee.

I have not submitted the record embodied in this Comprehensive report for the award of any other degree or diploma in any other institute.

Date: 7th May 2018 **Sudhir Kumar Verma**

Place: Roorkee (15541020)

CERTIFICATE

This is to certify that the above statement made by the candidate is correct to the best of my knowledge and belief.

(Dr. Anil Kumar)
Associate Professor
MIED, IIT Roorkee
UK-247667, INDIA

Acknowledgements

I wish to affirm my earnest acknowledgement to my respected guide **Dr. Anil kumar**, **Associate Professor,** Department of mechanical and industrial Engineering, Indian Institute of Technology Roorkee, for their intuitive and meticulous guidance and perpetual inspiration in completion of final dissertation. I want to express my profound gratitude for his co-operation in scrutinizing the manuscript and his valuable suggestions throughout the work.

I would like to mention my parents for their endless support and encouragement and always believing and helping me to believe, that I can succeed at anything.

Acknowledgement would be incomplete without a word of gratitude to all my student friends for their timely help, encouragement and contribution in making it possible.

Dated: 7th May, 2018

SUDHIR KUMAR VERMA

Place: Roorkee Enrolment No. 15541020

Abstract

One of the necessary features for the successful operation of a refrigeration unit is that the heat transfer performance of the refrigerant within the evaporator. The optimum design of the evaporator depends on the right analysis of the nucleate boiling and also the convective contributions to heat transfer. Nucleate boiling heat transfer is a widespread industrial process. The importance of nucleate boiling arises from its ability to get rid of huge quantities of heat per unit time and area from the hot surface with a comparatively low thermal temperature difference. Suggest that a tremendous reduction in heat exchanger surface is likely by means of nucleate boiling.

The thesis describes the results of an experimental investigation on nucleate pool boiling heat transfer of pure fluid R-134a and new environmentally harmless azeotropic refrigerant mixtures of R-125, R-143a, and R-134a (R-404a) on a plain horizontal copper Tube. The experiment has been carried out at saturation temperatures of $21^{o}C$ and heat fluxes from 5 to $40kW/m^2$ with an interval of $5kW/m^2$ in the increasing order of heat flux. The diameter of the test tube was 25.4 mm (1 in.) and had an effective length of 130 mm. Experimental data were compared with some empirical correlations available in the literature. The Jung, Cooper and Gorenflo correlations were well balanced with the present data of both refrigerants at given saturation temperatures. The Jung correlation under-predicts the experimental data with a maximum mean error of 11% for R-134 and 20-25% for R-404a while Cooper's under predicted the data of R-134a by 11% and 15% for R-404a.

Contents

List of figures

List of Tables

Nomenclature

d – bubble departure diameter, [m]

g – gravitational acceleration, [ms^{-2}]

h –boiling heat transfer coefficient, [$Wm^{-2}K^{-1}$]

k – thermal conductivity, [$Wm^{-1}K^{-1}$]

M – molecular weight, [$gmol^{-1}$]

n– exponent in Gorenflo correlation

P – pressure, [kPa]

Pc – critical pressure, [Psig]

P_r –prandtl number

p_r – reduced pressure, P/P_c [–]

q – heat flux [$Wm^{-2}K^{-1}$]

R_p – roughness, [mm]

T – temperature, [K]

ΔT – temperature difference, [K]

Greek letters

ϕ – contact angle, [deg.]

ρ– density, [kgm^{-3}]

ν – kinematic viscosity, [m2s–1]

σ – surface tension, [Nm^{-1}]

Subscripts

c – critical

sat – saturation

l – liquid

v – vapor

CHAPTER 1

1 Introduction

Nucleate pool boiling of refrigerants is a very important space of two-phase flow heat transfer as it is highly efficient in transferring the heat and having a large area of application in the industries like nuclear reactors, thermal power plants, refrigeration plants, space application, etc. It has a significant role in evaporator tube design where the best surface-liquid combination is required for better efficiency in transferring the heat. Nucleate pool boiling phenomenon has attracted considerable research and practical attention, due to its ability to transfer large amounts of heat with relatively small temperature differences. Therefore, if we tend to cut back the temperature difference in an evaporator or a condenser by one °C, it leads to rising an energy potency of somewhere within the variation of 2-4% based on the Carnot efficiency. Considering that a five-degree reduction might save us up to twenty percent of energy consumption, one can enhance the performance of a device operated as boiler, and even more with the proper structuring of its surface. Such structure ought to reduce the driving temperature difference what is achieved, generally by increasing the nucleation sites density. Originally, structures are generated by the mechanical machining, like by making completely different kinds of micro-fins and cavities within the heating surface, that increases the nucleation sites density and further, bubble detachment frequency. In enhanced boiling heat transfer, the temperature variations in evaporators are reduced through various ways, which leads to a rise in heat transfer. For the present research, we performed a comprehensive experimental study on pool boiling mechanism and surface effect on heat transfer enhancement. We have operated on a defined experimental set-up with a proper procedure, good-enough for locating heat transfer coefficient.

1.1 **Pool boiling Heat Transfer**

Nucleate boiling is a boiling method that takes place when the surface temperature is more than the saturated temperature of liquid by a certain amount but where the heat flux is below the critical heat flux Faghri et al. [1]. Heat flux (q") is plotted against the excess temperature ($\Delta T = T_w - T_{sat}$) in a typical boiling curve. With the increase in excess temperature, the pool boiling curve traverses in four different regimes namely, natural or free convection, nucleate boiling, transition boiling, and film boiling. A typical pool boiling curve of a saturated liquid at atmospheric pressure is represented in Fig. 1.1 where heat flux (q") is plotted against the excess temperature ($\Delta T = T_w - T_{sat}$) for a temperature-controlled environment.

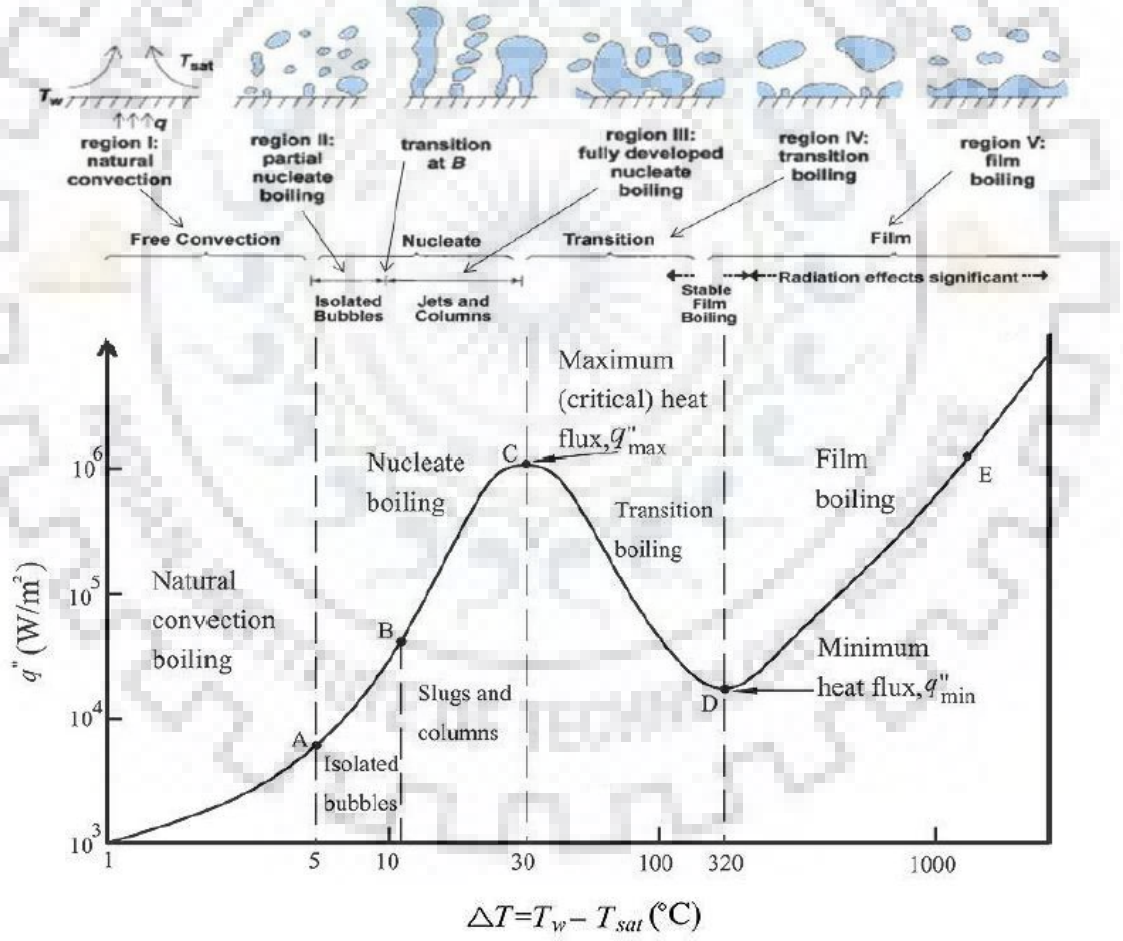

Fig. 1.1: Boiling Curve of a saturated liquid in a temperature-controlled environment.

There are criteria defined for the excess temperature (ΔT) which are: If excess temperature is less than 5°C, there is total absence of any bubble and only heat is transferred from the solid surface to the bulk liquid with the process of natural convection. If the excess temperature is more than 5°C for water, the curve enters into the nucleate boiling regime. In this scenario, the semi-empirical correlations for natural convection are being used for the calculation of heat transfer coefficients in this regime as discussed by Faghri et al. [1].

On point A of Fig. 1.1, vapour bubbles are generated at preferred locations on the heater surface which are known as nucleation sites. Nucleation sites are identified as microscopic cavities or cracks on the solid surface. Nucleation occurs repeatedly from these microscopic cavities or cracks, showing a link between bubble formation and some surface feature as well as the cyclical nature of the bubble-forming process Faghri et al. [1]. The reasons behind the bubble generation on small cavities and surface cracks are discussed by Faghri et al. [1] and are because of:

(1) The increase in the contact area between the liquid and heating surface compared to a relatively or perfectly-smooth surface, hence liquid trapped in cracks/cavities vapourizes first.

(2) The generation of liquid-vapour interfaces due to the presence of trapped gases in the cracks/cavities where the transfer of energy in the form of latent heat from the liquid to the vapour phase takes place.

The start of the formation of a vapour bubble under the right conditions at a nucleation site, further increase in the diameter of the bubble and attaining a defined size to detach from the heating surface and rises to the liquid free surface Faghri et al. [1].

As shown in Fig. 1.1 between point A and B, a bubble can grow and detach from the surface independently only if the excess temperature is and remains at the low end of the nucleate boiling regime. As the bubble-generating process occurs at the active nucleation sites, the surface area between these sites retains the liquid-solid contact that characterizes the natural

convection regime. Convection is always considered as the primary mechanism of heat transfer in 'isolated bubble' regime and the character of this convection is noticeably different from natural convection encountered at lower excess temperatures as discussed by Faghri et al. [1].

With the increase in excess temperature beyond the point B in Fig. 1.1, more activation of additional nucleation sites leads to more generation of bubbles. As the number of the bubbles increases in the system, the interaction among the bubbles further causes the merging of the bubbles, hence forming the columns and slugs of vapour. This leads to the decrease in the overall contact area between the heating surface and the saturated liquid in the system. Therefore, the slope of the boiling curve drops down and the heat flux reaches its maximum.

The rate at which bubble generate exceeds the rate at which bubble detach from the heater surface only if the temperature increases beyond the critical heat flux. With the rapid increase in bubble formation, continuous vapour films over the heater surface are getting generated, hence the fall in the contact area between the heating surface and the saturated liquid. It is very clear that continuous vapour films are not stable but they can detach from the heating surface and hence result in the further increase in contact area between the heating surface and the saturated liquid and again continuation with the nucleate boiling. With these defined rapidly fluctuating temperature conditions over the surface, the excess temperature should be taken into consideration as an average value (excess temperature shown on the ΔT-axis of Fig. 1.1). In this portion/regime of the curve where the boiling combines unstable film boiling with nucleate type, the boiling is referred to as transition boiling. To sustain a stable vapour film, the excess temperature should be high enough and the heat flux must reach its minimum value (point D).

The point D of the curve is known as the Leidenfrost temperature. It shows the upper-temperature limit of the transition boiling regime. Leidenfrost temperature is considered as a critical value in the system as if the temperatures are above it, the bulk liquid and the heating surface is completely separated by a stable vapour film. This type of boiling in this regime is called as film boiling. It is differed from the nucleate boiling as the phase change in film boiling occurs at a liquid-vapour interface whereas in nucleate boiling it takes place directly on the surface. Pool boiling remains active in this regime until the surface temperature reaches the maximum allowable temperature of the heating surface.

1.2 Types of Pool Boiling and Heating Methods

Some important parametric effects on the pool boiling curve can be described.

With the increase in surface wettability (reduction in contact angle), the nucleate boiling line shifts towards right. Therefore, increase in surface wettability leads to decrease in nucleate boiling heat transfer coefficients (for the same Tw − Tsat).

Increase in surface wettability leads to the increases in the maximum heat flux. Liquid pool sub-cooling effect on fully developed nucleate boiling region is small whereas it improves the heat transfer in all other boiling regimes, as depicted in Fig. 1.2. The choice of heating methods is shown in Fig. 1.3 places constrain on the material and the thickness of the heated wall, which may not match the conditions in industrial systems. The role of bulk properties of the wall is overshadowed by the influence of condition of its surface.

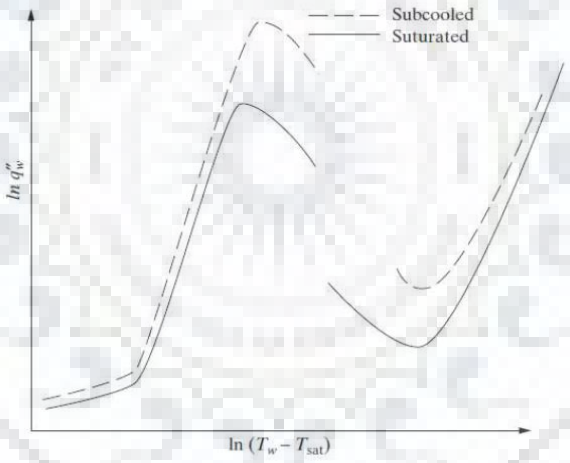

Fig. 1.2: The effect of liquid pool sub-cooling on the boiling curve.

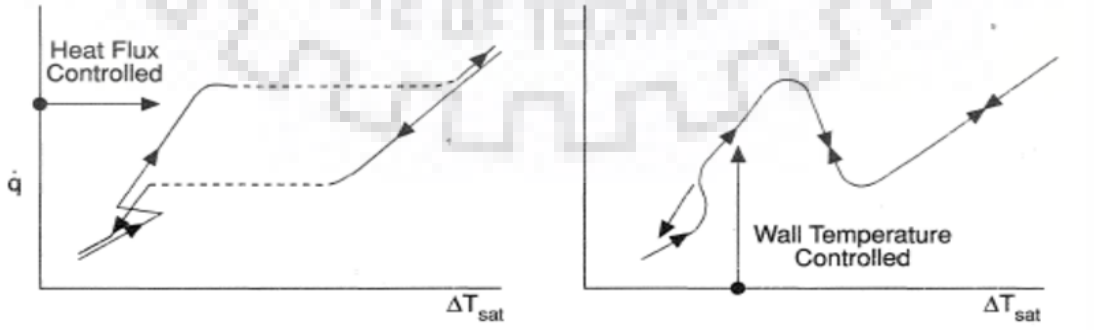

Fig. 1.3: Effect of heating method on boiling curve.

1.3 Nucleate Boiling Heat Transfer Mechanisms

The following are the main identified heat transfer mechanisms playing a role in nucleate pool boiling as illustrated in Fig. 1.4:

1.3.1 Bubble agitation

Bubble agitation is a dependant on the intensity of the boiling process. It is the process in which the systematic pumping motion of growing and moving bubbles agitates the liquid by pushing it back and forth across the heater surface. This agitation of liquid transforms the natural convection into forced convection, locally speaking. Sensible heat is transported away in the form of superheated liquid Bejan & Kraus [2].

1.3.2 Vapour–liquid exchange

A cyclic thermal boundary layer stripping process is created by the removal of the thermal boundary layer from the heated surface due to wakes of departing bubbles. In this process, sensible heat is transported away in the form of a superheated liquid and it is also dependent on the intensity of the boiling process. The rate of removal of bubbles whose rate of removal is proportional to the thickness of the layer, its mean temperature, the area of the boundary layer removed by a departing bubble, the bubble departure frequency, and the density of active boiling sites.

1.3.3 Evaporation

This process is divided into two: Macro evaporation and Micro evaporation or Micro layer evaporation. Macro evaporation happens over the surface of the bubble whereas micro layer evaporation happens underneath the bubble across the thin liquid layer trapped between the bubble and the surface. The heat is conducted firstly into the thermal boundary layer and then to the bubble interface, where it is converted to latent heat. Latent heat is generated by the

conducted heat into the bubble interface. Heat is also conducted into the thermal boundary layer. Volumetric flow of vapour is important as the rate at which the latent heat transport is directly dependent on the volumetric flow of vapour away from the surface per unit area.

With thermal consideration, the above discussed mechanisms compete for the same heat in the liquid and hence overlap with one another. Isolated bubble regime is characterized by low heat flux. In isolated bubble region/regime, natural convection happens even in inactive area of the surface where no bubbles grow.

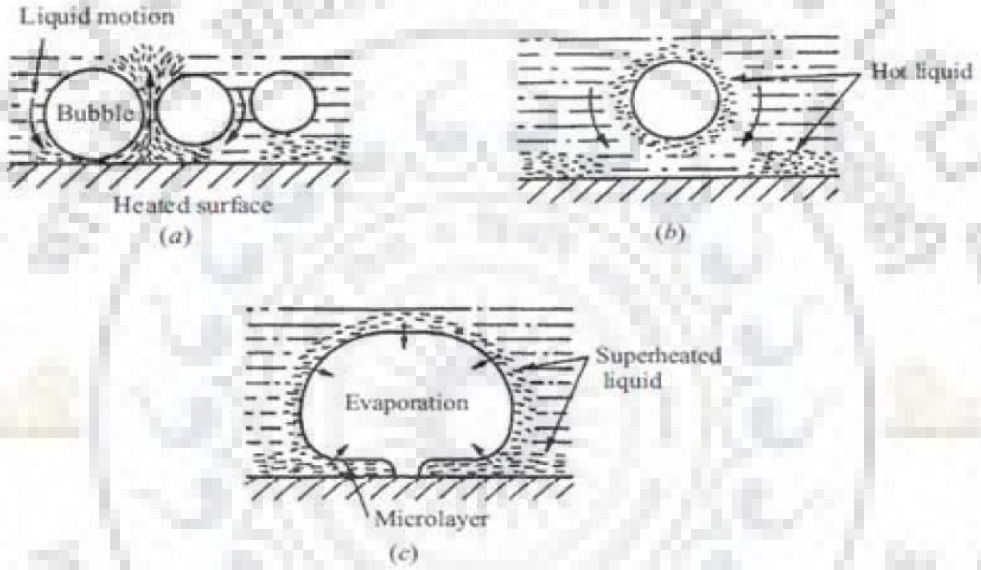

Fig. 1.4: Heat transfer mechanisms in nucleate pool boiling: (*a*) bubble agitation; (*b*) vapour–liquid exchange; (*c*) evaporation.

1.4 **Boiling enhancement**

As a known fact, the nucleate boiling on a plane surface occurs at a substantial wall superheat. Over the years, numerous efforts have been devoted to reduce the temperature difference between the heated wall and the boiling liquid, known as the wall superheat, by different means and techniques. Work as such has been commonly termed in literature as boiling enhancement. An enhanced boiling surface is expected to initiate nucleate boiling at a minimal wall superheat and sustain it at low heat fluxes. Ideal enhanced surface should address both these issues. In practice, some surfaces were proved to be rich in one aspect but poor in the other.

When the performance of an enhanced surface deteriorates with time, that effect is termed 'aging'.

Interaction on a heated surface as illustrated in Fig.1.5:

1: Thermal interaction between bubble and heated surface.
2: Thermal interaction between nucleation sites.
3: Hydrodynamic interaction between bubble and liquid bulk.
4: Hydrodynamic interaction between bubbles.

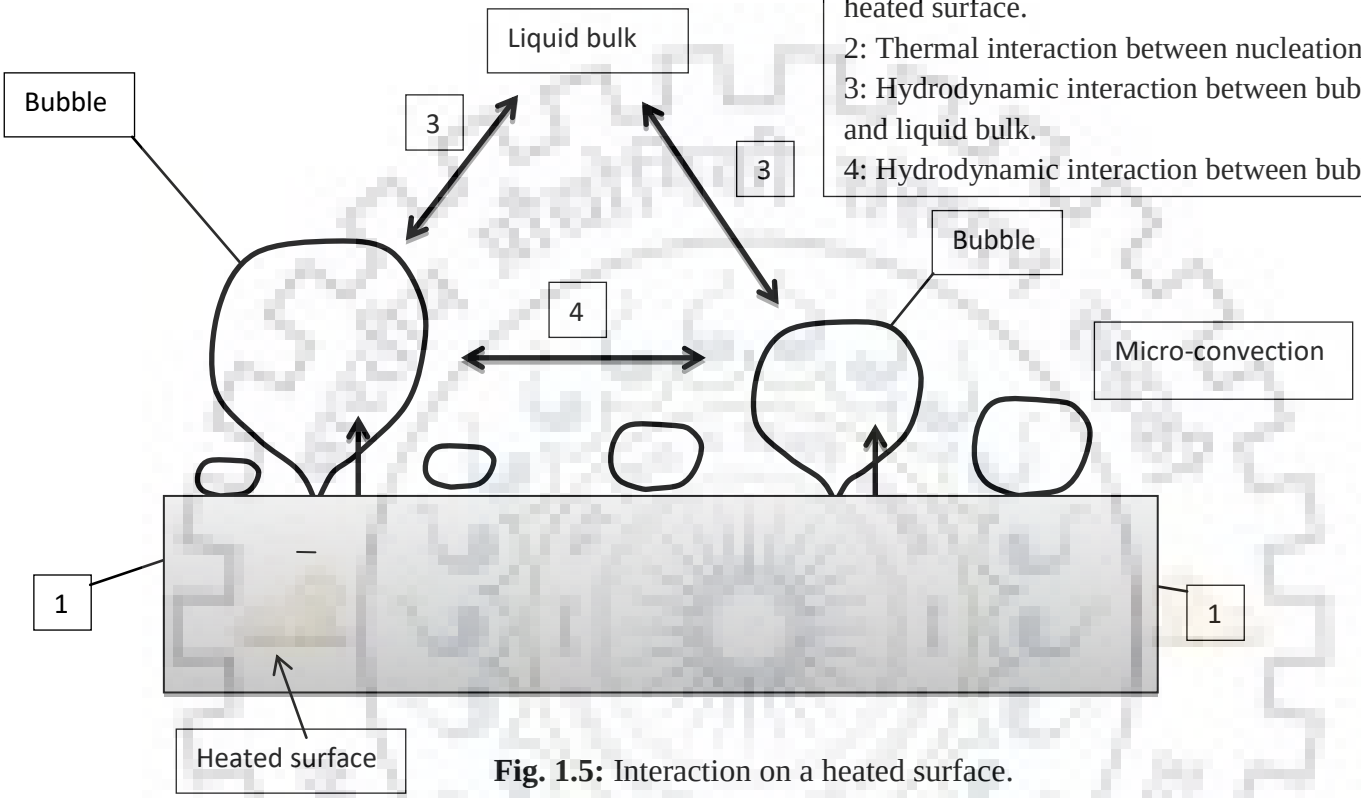

Fig. 1.5: Interaction on a heated surface.

1.4.1 The motive for boiling enhancement

In the earlier discussion, it was also stated that the heat flux per unit wall superheat is substantially large in the nucleate boiling regime. This proves the fact that the heat transfer coefficient is higher in nucleate boiling. Consider a two-fluid counter flow heat exchanger. The rate of heat transfer from the cold fluid to the warmer fluid would be expressed as,

$$Q = U.A.\ (\Delta T)_m \qquad (1.1)$$

The term U stands for the overall heat transfer coefficient, which may also be expressed as a summation of convection terms for the two fluids and conduction term for the surface,

$$\frac{1}{UA} = \frac{1}{(hA)_1} + \frac{\delta}{kA} + \frac{1}{(hA)_2} \quad (1.2)$$

A 'good' heat exchanger would display a higher *U* value. Practical significance of a high *U*-value may be exploited in 3 ways,

- For a given *Q* and the area *A* unchanged, the mean temperature difference between two fluids *(ΔT)* m may be reduced. Primarily, this would reduce the system operating costs.
- For a given *Q* and *(ΔT)* m unchanged, the heat exchange area could be reduced. Consequently, the size of the heat exchanger would become small.
- While keeping the area *A* and temperature difference *(ΔT)* m unchanged, the rate of heat transfer *Q* may be increased.

1.4.2 Enhancement techniques

Surface enhancement technology in recent years has been highly focused on the improvement of two phase heat transfer that is the transfer of thermal energy due to the phase transformation from the liquid to the vapour phase. Methods to improve the two-phase heat transfer may broadly be classified into two groups:

Passive techniques:

This technique represents those that do not require an external source of power. They include treated surfaces, rough surfaces, extended surfaces, displaced enhancement devices, swirl flow devices, coiled tubes, surface tension devices, additives for liquids, additives for gasses.

Active techniques:

This technique in contrast, needs external power and they include mechanical aids, surface vibration, fluid vibration, electric or magnetic fields, injection or suction, jet impingement and compound techniques.

1.4.3 Boiling on enhanced surfaces

A liquid boiling on a surface may release the heat in two forms: first, it may leave as latent heat in the releasing vapour bubbles and second, as sensible heat in the superheated liquid rising from the surface. The difference between the boiling mechanism on a plane surface and on an enhanced surface is that in the latter case, the degree of enhancement follows the surface geometry. This makes a particular surface geometry better or worse in performance than the other. In addition to the inherent advantages associated with nucleate boiling on a plane surface, the further augmentation in boiling on an enhanced surface may be attributed to:

(a) Latent heat in vapour formed within the enhancement matrix,
(b) Evaporation in bubbles emerging from the enhancement matrix, and
(c) Superheating of the liquid pumped into and out from the enhancement matrix

There are many techniques which are used for enhancing boiling on tubes and are summarized here in Fig. 1.6. A lot of research has been carried out and these recently developed surfaces are identified which greatly enhance the boiling heat transfer. These surfaces allow, first of all, boiling to occur at lower wall superheats and ultimately reduce the physical size of these heat exchangers.

When these surfaces are utilized on industry scale, they are supposed to be robust and technically sound. There are some examples given of widely used enhanced surfaces which are commercially available and are shown in Fig. 1.7. Instead of a lot of literature, a full-proof understanding about the mechanism of boiling on enhanced surfaces does not exist. Two basic types of enhanced surfaces namely, porous and structured are identified and exist. It has been found that the structured surfaces are better to be used in analyses as description of the boiling mechanism could be inferred more appropriately than in the porous surfaces. The reason behind is the knowledge of well defined dimensions in case of structured surfaces compared to the irregular geometry of the porous surfaces.

To attain high boiling performance, three concepts are employed generally which are as follows:

1. Use of re-entrant tunnel-type cavities.
2. To reduce the superheat (must requirement), the subsurface pores needs to be significantly larger than those happens to be present on natural surfaces.

3. Supply of the liquid to the subsurface as capillary passages via the surface pores. As the liquid proceeds through the capillary passages, the liquid is heated and thin film evaporation occurs from liquid vapour interfaces in the subsurface capillaries.

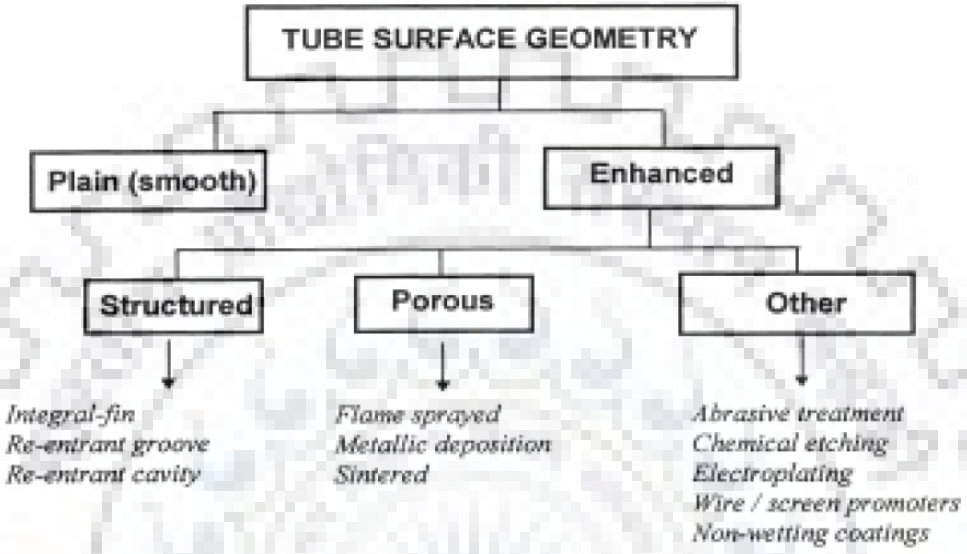

Fig. 1.6: Diagram highlighting the different tube surface geometries.

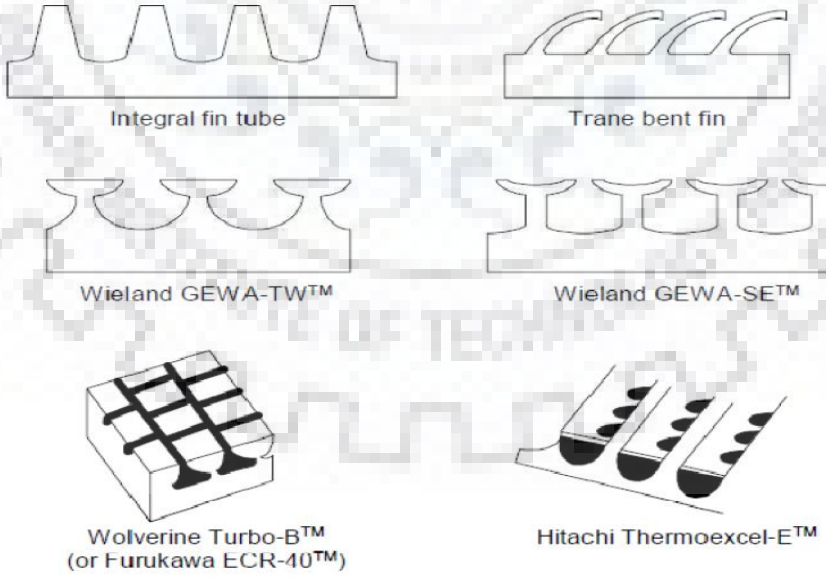

Fig.1.7: Examples of commercially available enhanced boiling surface.

CHAPTER 2

2 Literature Review

2.1 Boiling on Plain Tube

Pool boiling experiments are conducted using smooth surfaces to characterize the boiling heat transfer coefficients of HFO-1234yf by Park and Jung [3]. They conducted their experiments at a saturation temperature of 7°C (Psat¼0.39 MPa) and did not reach the CHF and reported that the nucleate boiling heat transfer coefficients of HFO-1234yf are similar to those of HFC-134a and can be predicted with reasonable accuracy using existing correlations. Further, Forrest et al. [4] investigated the effect of pressure on pool boiling heat transfer using HFC-134a as the working fluid in a more recent study. Forrest et al. [4] have conducted these tests at saturation temperatures of 25°C and 50°C using a 2.54 cm diameter copper tube heater and concluded that with the increasing pressure, nucleate boiling heat transfer coefficients and CHF increases. In other study Se´rgio Pereira et al. [5] conducted the nucleate pool boiling of R134-a on plain, and micro-finned copper tubes was investigated through experiments performed at pressures between 6.1 and 12.2 bar. Se´rgio Pereira et al. [5] has concluded that the heat transfer coefficient is higher for the micro-finned tube than for the plain tube based on their experimental results. All these enhancements of the heat transfer due to the fins discussed so far are only notable at sufficiently high heat flux and on the bottom part of the tube. The mechanism behind phenomenon is proposed to be caused by the large bubbles growing on the bottom part of the tube, while on the plain tube a dried area appears at the foot of these bubbles. Some liquid is trapped in the fins enable a stronger heat transfer at the bubble foot on the micro-finned tube.

2.2 Boiling on Enhanced Tube

The major results are available to the study the boiling on enhanced tube. There are a number of different techniques which are employed to enhance the pool boiling heat transfer rates. These techniques include surface roughness, coated surfaces, re-entrant cavities, and

finned surface. Among all these four employed techniques, use of re-entrant cavities technique is widely studied for enhancement of heat transfer in the literature.

2.2.1 Surface roughness

This criterion is being employed by many workers and the conclusion drawn is that surface roughness and tube orientation have a small effect on the heat transfer enhancement. Experiments have been conducted by varying the average roughness on the boiling surface by pioneer worker like Hsieh and Yang [6] and Ribatski and Jabardo [7]. Hsieh and Yang [6] and Ribatski and Jabardo [7] have reported slight enhancements in the heat transfer performance for higher average roughness surfaces based on their experimental results. Adding to the existing literature, Kang [8] in 2003 performed a series of experiments by varying the inclination angle of the tube from horizontal to vertical orientations in steps of 15°C. Kang [8] has used water as the working fluid over a stainless steel cylindrical surface and found a relative enhancement of up to 1.4 times at an inclination of 15°C from the horizontal. Based on his results, he further concluded that the reduced bubble slug formation at the bottom surface of the tube was due to the slight inclination. In this series, Chien and Webb [9] found a better heat transfer performance in horizontal orientation in comparison of vertical orientation.

2.2.2 Coated Surfaces

a) Conductive metal coatings

The advantage of thermally conductive metal coating is its high thermal conductivity due to which it gives more enhancement of heat transfer compared to non-metal coating. A significant advantage of this conducting micro-porous coating is insensitivity of coating thickness due to the high thermal conductivity of solder binders. In addition, the coating technique is efficient for various types of working liquids simply by changing the size of metal particle sizes since different surface tension of liquids requires different sizes of porous cavities to optimize boiling heat transfer performance.

b) Non-metal coatings

Non-metal coatings are defined as the micro-porous coatings that employ epoxy-type materials with low thermal conductivity to bind metal particles. ABM coatings were previously developed and patented by You and O'Connor [10]. The micro-porous coating yields a boiling

enhanced surface by increasing vapour/gas entrapment and active nucleation site density with a porous structure. The coatings are named from the initial letters of their three components. ABM coating is made up of **A**luminum, Devcon **B**rushable Ceramic, and **M**ethyl-Ethyl-Keytone and is thermally non-conductive because Brushable Ceramic is an epoxy-type binder with low thermal conductivity (less than 1.0 W/mK).

Enhancement of the boiling heat transfer is directly depending on the number of active nucleation sites. The porous surfaces provide higher number of nucleation sites; hence a porous surface over the heated tube is preferred as a technique to be utilized for the enhancement of the boiling heat transfer. Several studies have also been conducted by the workers like Hsieh and Yang [11] in 2001 where they have studied the heat transfer mechanism in a porous layer matrix. Hsieh and Yang [11] are credited towards the confirmation of the earlier hypothesis of nucleation and evaporation taking place in the porous matrix under steady boiling conditions. Further the advancements have been done over the topic where Cieslinski [12] have conducted an extensive parametric study. He has utilized porous layer coatings of different materials such as copper, aluminum, molybdenum, zinc and brass for the enhancement of the boiling heat transfer. Water was used as a working fluid media and the conclusions were drawn as aluminum coatings give the highest heat transfer enhancement. One of the other observation, he has made is that the boiling process starts at much lower wall superheats (approx. 0.1 K) with the porous layer coatings compared to a smooth tube where the boiling starts at 8 K. Further in the series, Kim et al. [13] have utilized a porous layer coating over a thin platinum wire for the enhancements and the results have shown an increase of up to 3.75 times. The reason they have discussed is that an increase in the bubbling frequency and the reduction in the bubble departure diameter with the porous layer coatings.

2.2.3 Re-entrant cavities

Trapped vapour in re-entrant cavities acts as nucleation sites and further takes part in the nucleation process. Re-entrant cavities augment the heat transfer performance by approximately 3–4 times. Four GEWA series tubes and a TURBO-B tube was tested by Webb and Pais [14] in 1992 and re-entrant cavities are generated over GEWA series tubes and a TURBO-B tube by by performing further processes on the finned tubes. Webb and Pais [14] have tested these surfaces with R11, R12, R22, R123 and R134a at saturation temperatures of 4 °C and 27 °C. These experimental results have shown that higher heat transfer coefficients are obtained at higher

saturation temperatures of 27 °C. Commercially available re-entrant cavity tubes: GEWA series, Thermo-excel and Turbo tubes were used for testing by Memory et al. [15] and an enhancement in heat transfer coefficient up to 5.5 times for the GEWA series tubes and up to 20 times enhancement for the Thermo-excel and the Turbo tubes was recorded with the condition of low heat flux. The higher the heat fluxes, the lower the heat transfer coefficients as shown by other similar tubes. By modifying the tips of the finned tubes, Rajulu et al. [16] have fabricated the simple re-entrant cavities and showed an enhancement of up to 2.5 times. They observed a comparatively slight drop in the enhancement factor with higher heat flux conditions and have also developed a correlation for the enhancement factor as a function of the heat flux and the cavity width of the re-entrant channels. Further, re-entrant cavity tubes with refrigerant and lubricant mixtures have been tested by Ji et al. [17] and based on their results they have found that narrower cavity mouth widths tubes performed better at low heat fluxes whereas wider cavity mouth widths tubes performed better at higher heat fluxes. Relatively poor enhancement factor was observed at higher heat fluxes. Re-entrant cavity surfaces by wrapping pored foils around the outer surface of finned tubes was developed by Chien and Webb [18] and further, they have performed a parametric study on the pore diameter, tunnel pitch, tunnel width, and fin height. The major conclusion of their study was that better performance could be obtained by greater fin height and a smaller tunnel pitch. To higher the heat transfer performance, finned tubes with rectangular bases and fin heights of 0.7–1.0 mm was suggested by them as they have found that the subsurface heat transfer was offered by the evaporation of the liquid filled in the corners of sharp-edged tunnels.

2.2.4 Finned Tube

Unmodified integral finned tubes have been tested and utilized for the enhancement in the heat transfer rates by various researchers [2 & 3]. Nakayama et al. [19] in 1980 have shown in their pool boiling experiments with R11, water, and nitrogen over flat surfaces that the wall superheat for a given heat flux could be reduced by 80–90% with the use of their porous re-entrant cavity surfaces compared to a plain surface. With the use of open microchannel geometries over flat surfaces with water as the working fluid Cooke and Kandlikar [20] have obtained higher heat transfer coefficients at a considerably higher heat flux (2.44 MW/m^2). Further they have concluded that wider and deeper channels with thinner fins

performed relatively better and the re-wetting of the heated surfaces through the open microchannel network and the bubble dynamics was the main reason responsible for the better performance.

Table 2.1: Summary table of the experimental results for various pool boiling heat transfer enhancement techniques over cylindrical surfaces.

Author/year	Material/diameter (mm)/ working fluid	Heat flux range (kW/m2)	Enhancement technique	Enhancement Factor	Comments and conclusions
Park and Jung et al.[3]/2010	Copper/HFO-1234yf/HFC-134a	2-30	Plain tube/finned surface	-	Nucleate boiling heat transfer coefficient of HFO-1234yf are similar to HFC-134a
Forrest et al. [5]/2010	Copper/2.54/HFC-134a	10-30	Plain tube	-	Increasing nucleate boiling heat transfer coefficient and CHF with increasing pressure
Se´rgio Pereira et al.[5]/2013	Copper/R-134a	10-100	Plain/micro-fined tube	-	At high heat flux, higher HTC for the micro-fined tube than plain tube
Ribatski and Jabardo [7]/2003	Copper, brass, stainless steel/19/255/R11, R12, R22, R123, R134a	0.6–120	Surface roughness	-	Possibly due to natural convection, an increase of active nucleation sites on the top surface of the tube compared to the bottom
Hsieh and Yang [11]/2001	Copper/20/210/R134a, R600a	0.1-30	Porous surface (with surface roughness)	1.2–2.3	Heat transfer enhancement due to the porous layer thickness and nucleation and vapourization took place inside the porous matrix
Chien and Webb [9]/1998	Copper/18–19.5/140/ Methanol	2-70	Re-entrant cavities (with pored foil) tube orientation	2.5	Vertical orientation showed 10–20% lower heat transfer rates compared to horizontal orientation
Kim et al. [13]/2002	Platinum/0.39/40/ FC72	Up to 400	Porous surface	6 (approx.)	An increase in latent heat transfer at low heat fluxes with the increase in convective heat transfer at high heat fluxes; Augmentation of the performance was through microporous coatings
Dominiczak and Cieslinski [12]/2008	Stainless-steel/8.15-23.60/250/ distilled water, R141b	.1-100	Porous surface	-	A fall in the average wall temperatures, Reduced the circumferential temperature; horizontal orientation by partially coating with porous layer coating on the top region of the tube

Webb and Pais [14]/1992	Copper/17.5 and 19.1/ 152.4/R11, R12, R22, R123, R134a	3–80	Re-entrant cavities Microchannels/integral fins	1.4-2 1.4-2	At a given heat flux, an increase in the heat transfer coefficient with an increase in saturation temperature
Memory et al. [15]/1995	Copper/15.9/190/ R114, R114 oil mixtures	.5-100	Re-entrant cavities Porous surface Microchannels/integral fins	2-20 3.6-18 1.7-4	With an increase in the heat flux, a steady performance drop for all the re-entrant cavity tubes and porous surface tubes
Rajulu et al. [16]/2004	Brass/33/218/ isopropanol, ethanol, acetone, water	11-42	Re-entrant cavities	1.2–2.65	Acetone and isopropanol performed well on higher cavity mouth widths of the tubes (0.3 mm), whereas ethanol and water performed well on the lower cavity mouth widths tubes (0.2 mm)
Ji et al. [17]/2010	–/18.50–19.09/1088–1100/R134a	9-90	Re-entrant cavities Microchannels/integral Fins	4 1.6	Narrower mouth widths of re-entrant cavity tubes performed well at lower heat fluxes whereas wider mouth widths of re-entrant cavity tubes performed well at higher heat fluxes
Chien and Webb [18]/1998	Copper/19.1/140/ R11, R123	2-70	Re-entrant cavities (with pored foil)	-	Higher heat transfer enhancements with greater tunnel height and smaller tunnel pitch; dry-outs in the tunnels at certain heat fluxes with the liquid depletion in the tunnels

2.3 **Parameters that Influence the Degree of Enhancement**

So far, the discussion has been mainly directed to the general aspects of enhancement techniques. From now onwards, it will gradually turn to the technical aspects of enhancement, concentrating on the influence of pressure, temperature, surface geometry and forces acting on bubbles. It is thought fair to introduce two correlations those are applied throughout the following text, in one or the other way. First on them is the Laplace equation. The Laplace equation correlates pressure in and outside a bubble, P_V, and P_l, to the surface tension forces σ and the bubble radius r.

$$P_v - P_l = \frac{2\sigma}{r} \tag{2.1}$$

The second useful equation introduced here is the Clasius-Clapyron equation. It expresses pressure difference in terms of the temperature difference.

$$\frac{dP}{dT} \sim \frac{h_{fg}\rho_v}{T_s} \tag{2.2}$$

Where hfg is the latent heat of vapourization, ρv is the density of vapour, and Ts is the saturation temperature. By combining these two equations, it is possible to derive a correlation, which shows liquid superheat (T_l-Ts) needed for a bubble of radius *r* to exist in a liquid.

$$T_l - T_s = \frac{2\sigma T_s}{\rho_v h_{fg} r} \tag{2.3}$$

2.3.1 The shape and the geometry of cavities

Griffith and Wallis demonstrated that the geometry of a cavity containing trapped vapour is directly related to bubble nucleation process. The mouth radius r_c determines the superheat needed to initiate boiling and the cavity shape determines the stability of vapour generation process. By using the Laplace and Clasius-Clapyron equations, they showed that the cavity mouth radius is inversely proportional to the wall superheat. A re-entrant cavity and a progressing vapour front are shown in figure 2.12. The re-entrant type cavity presented by them

was further investigated by Benjamin et al. and proved excellent performance. However, Yatabe observed that the interior shape of re-entrant cavities does not influence its performance. It is also important to trap the vapour in the cavities so that the cavities do not become inactive after some time.

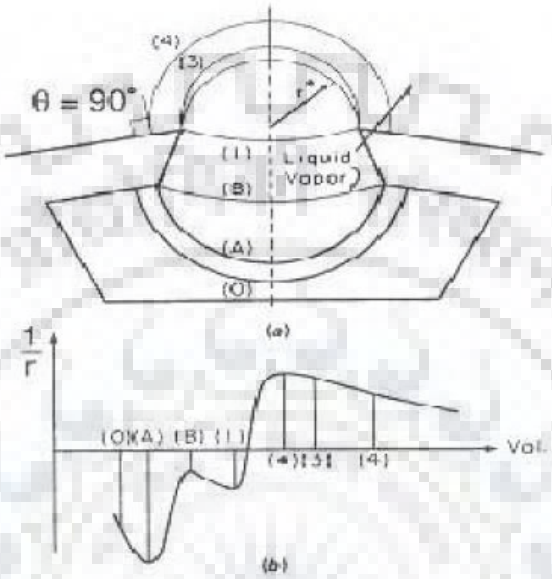

Fig. 2.1 (a) Liquid-vapour interface propagation in a re-entrant cavity. (b) Reciprocal of interface radius vs. vapour volume for a liquid with a 90° contact angle

Webb investigated the liquid superheat requirement for a stable vapour front to existing in five different cavity shapes with the same mouth radius r_c for a liquid contact angle θ of 15°. Depicted in figure 2.2 are the cavity shapes those came under consideration and the results of the analysis. The following conclusions were drawn; the liquid superheats required for a vapour bubble to exist at the cavity mouth did not significantly vary between cavity shapes; the re-entrant cavities required the smallest liquid superheats to exist within the cavity; and if the sub cooled liquid were introduced into the cavity, only the shapes D and E would be stable. In a practical point of view, more interesting is to establish the degree of wall superheat needed for a bubble to exist on a given cavity. Consider the case where the bubble radius is equal to the cavity mouth radius, i.e., r= r_c. For a curved liquid-vapour interface of radius r to exist in a liquid, there has to be a certain minimum liquid superheat (T_1-T_s). This can be written as;

$$T_l - T_s = \pm \frac{2\sigma}{mr} \qquad (2.4)$$

Where T_l and Ts are respective temperatures of liquid-vapour interface and saturation. And, m is the local slope of the saturation curve (Ps - Ts), which by approximating to Clasius-Clapyron the equation gives $m = \frac{h_{fg}\rho_v}{T_{abs}}$. Further, the choice of the sign, + or -, is chosen depending on if the shape of the liquid front is concave or convex.

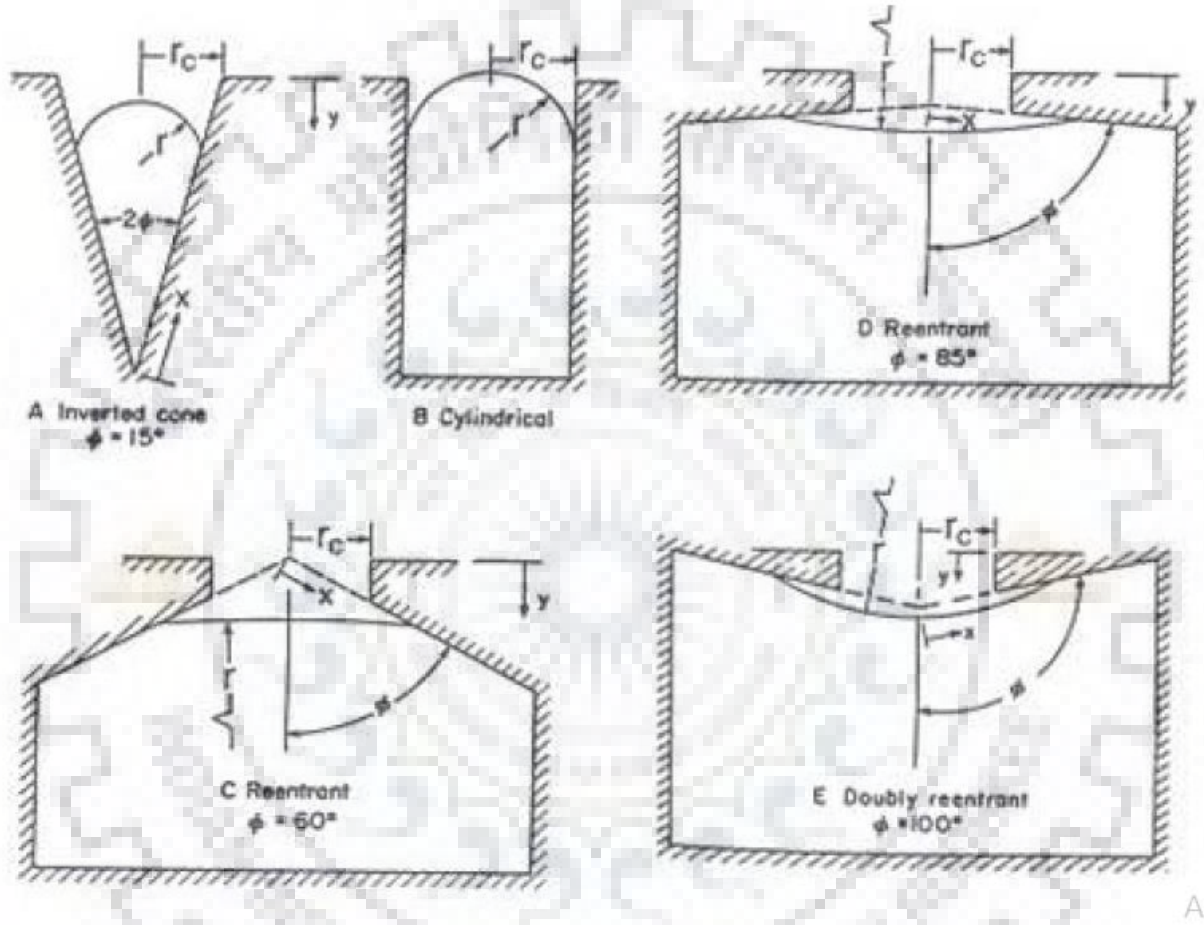

Fig. 2.2: Vapour-liquid interface radius in cavities of different shapes with r_c = 0.04mm, θ =15°

2.3.2 The nucleation site density

Researchers have attained a relationship between heat transfer coefficient and also the nucleation site density; h α $(N/A)^{0.43}$ and further developed the subsequent correlation that displays the relationship between the boiling heat flux, wall superheats, liquid properties and the surface conditions.

$$\dot{q} = 2[\pi(k\rho c)_l f]^{\frac{1}{2}} d_b{}^2 N(\Delta T) \qquad (2.5)$$

They determined the bubble departure diameter d_b from,

$$d_b = C_1 \left[\frac{\sigma g_0}{g(\rho_l - \rho_v)}\right]^{\frac{1}{2}} (Ja)^{5/4} \quad (2.6)$$

Where, $\mathbf{C_1}$ is an empirical constant for the boiling liquid, and the modified Jacob number $\mathbf{J_a}$ is given by,

$$J_a = \frac{\rho_l c_1 T_s}{\rho_v h_{fg}} \quad (2.7)$$

Now, by knowing d_b, the bubble departure frequency f was determined from,

$$f d_b = C_2 \left[\frac{\sigma g_0 g(\rho_l - \rho_v)}{\rho_l^2}\right]^{1/4} \quad (2.8)$$

Where, C_2 was a constant drawn upon experimental results, and g_0 is a conversion factor given by the authors the value 4.17*108 lbmft/hr2lbf. Nukiyama et al. justify how to determine these entities. Chien and Webb [9] conducted studies on bubble dynamics on an enhanced boiling surface like a Hitachi Thermo Exel-E tube. Among his conclusions was that the nucleation site density increases as the heat flux increases.

2.3.3 The base surface thermal conductivity

A number of researchers mentioned in the preceding text had commented on the influence of the thermal conductivity of the base surface to its heat transfer performance. They found either little or no distinction in performance between a base surface with high conductivity particles and that of a comparatively low conductivity. Mann et al. ensure this concept after performing a mathematical simulation to examine the influence of the wall (the base surface) thermal conductivity and liquid properties upon boiling heat transfer. Within

the study, they boiled R-114 on totally different surfaces with various thermal conductivities. They kept all alternative parameters including bubble site density was maintained constant throughout the tests. Shown in table 2.2 is a comparison of heat transfer coefficient for boiling on surfaces made of three different materials. Their conclusion was that a large variation of wall thermal conductivity has an only moderate influence on heat transfer to a growing vapour bubble.

Table 2.2 Boiling R-114 on surfaces with different thermal conductivities.

Wall Material	$\Delta T\ (K)$	$\dot{q}(W/m^2)$	h (W/m^2K)
Copper	4.48	5000	1116
Steel	4.48	4910	1095
Ceramics	4.48	4026	898

2.4 Gap in literature

During literature survey, following gaps has been identified for the current research:

- Up to now, no research efforts on the nucleate boiling heat transfer enhancement of R-404a have been reported over finned surface in open literature.
- A very few research has been done for pool boiling over horizontal finned tubes.
- Few works have been analyzed for the effect of the finned surface over horizontal single copper tubes on the heat transfer coefficient.

2.5 Objectives of the current research

The main objective of the present work is to evaluate enhancement in the heat transfer coefficient performance of a R-134a and R-404a refrigerants on modified tube surface which includes-

1. Design and fabrication of the test surface of copper tube.

2. To determine the thermal performance of modified tube over plain tube like heat transfer coefficient, wall superheat.
3. To compare the experimentally obtained values of heat transfer coefficient and wall superheat with the existing correlations for plain tube and also compare with enhanced tube surface.

2.6 **Organization of the Thesis**

The present thesis is the compilation of the results of research carried out during 2015-16 and it is divided into five chapters for better representation of the work. The chapters include:

Chapter 1: In this chapter, a general introduction to the pool boiling has been given and the scope of the future work is discussed.

Chapter 2: This chapter represents a compilation of the literature studied for the identification of research problem and its scope. Emphasis has been given to the literatures related to the methods utilized for enhancement of heat transfer coefficient over various modified surfaces of copper tube.

Chapter 3: A detailed description of the experimental setup has been given in this chapter. The design and fabrication of tube surface has been included in this part of the thesis.

Chapter 4: Obtained results from the experimental set-up are presented in this chapter along with the critical evaluation of these results with the available literature.

Chapter 5: This chapter is devoted to the concluding remarks for the current research and scope for future work is discussed.

CHAPTER 3

3 Experimental Set-up

The basic experimental set-up utilized in the present study consisted of mainly an evaporator along with a condenser as depicted in the Fig. 3.1. Broadly, the experimental set-up included: refrigerant and coolant and water circulating loops. The mechanism could be explained like: the refrigerant vapour boiled off the heat transfer tubes, further went into the condenser, and then condensed there. The liquid was fed to the evaporator by gravity. To keep-up the pool temperature at a specific saturation temperature, the coolant water came from the external chiller within the condenser. A stainless-steel pipe of one hundred fifty millimeter inside diameter and 495 millimeter length was used as an evaporator.

CNC lathe machine was used on sleek copper tubes for the micro-finned test tube fabrication. The test tube will be mounted on the SS flange at one end of the test cell, and the sight glass has been installed on the opposite end of the test cell. The vapour generated during the test will be condensed within the internal condenser. The enhanced tubes are specially made up of thick walled copper tubes of 25.4 millimeter outer diameter and 20.2 millimeter inner diameter. The length is 150 millimeter. An electrical cartridge heater of 20 millimeter diameter and 180 mm long will be inserted into the test tube. Its electric power was controlled by a power variac. Calibrated T-type thermocouples will be used to measure the temperatures of the refrigerant, and the outside surface of the test tubes. The boiling surface temperature and heat flux are going to be determined from measured temperature by assuming one-dimensional heat conduction. One thermocouple will be placed in the boiling vessel and one in the vapour house. The saturation state (10 to 20 ^{0}C) will be confirmed by observance the liquid and vapour temperature throughout the experiments. The vapour is condensed within the water-cooled condenser. The condensate will be returned to the vessel to maintain a constant saturation temperature within the vessel. The pressure in the boiling vessel is going to be measured by a pressure gage. Temperature data will be recorded by a computer-controlled Adam 4000.

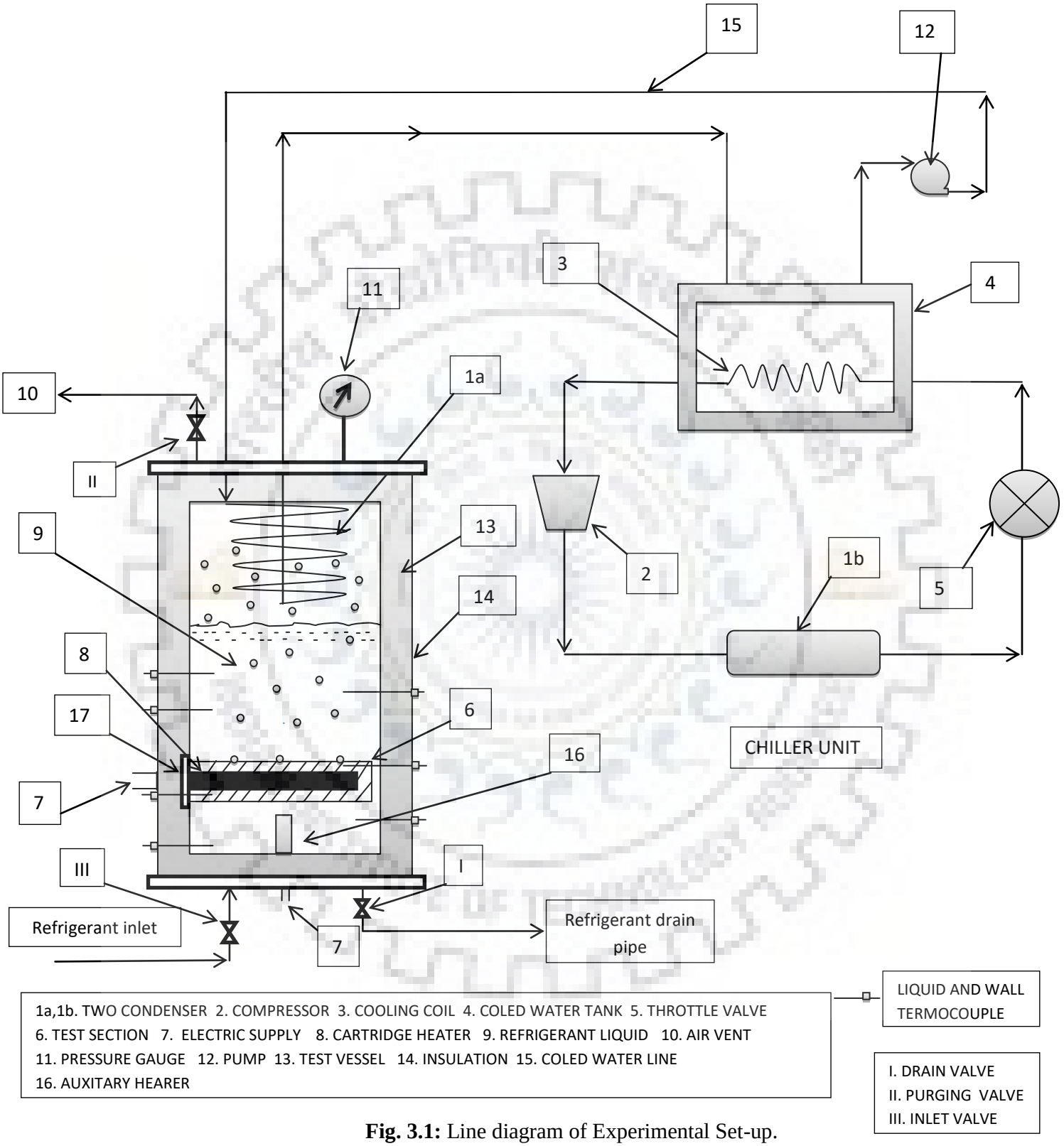

Fig. 3.1: Line diagram of Experimental Set-up.

3.1 **Line diagram of experimental setup**

Experimental facility as shown in line diagram is composed of a test vessel {13} to hold the boiling liquid; a copper tube as heating surface {6}; a cartridge heater {8} and an auxiliary heater {16}; condenser {1a} condense back the vapours of the boiling liquid and second condenser {1b} uses in chiller plant; and instruments to measure the temperature & pressure; the electrical energy input to the heating copper tube, and vacuum in the test vessel. In a cylindrical vessel {13} of stainless steel, having top and bottom cover with a disc shape, drain valve {I} is attached for draining out the test liquid from the vessel. The top cover has various fittings for pressure gauge {11}, condensers {1a}, and test liquid inlet line. The vessel has two inspection windows diametrically opposite to each other with glasses through which one can see the vapour bubble dynamic on the tube surface and the liquid pool around it. Sockets {17} weld to the body of the vessel, help in placing the copper tube in the vessel for its horizontal orientation in the liquid pool. The vessel body except the top flange is thermally insulated with asbestos rope. The tube made out of copper rod with required dimension. Inside the tube, a cartridge heater is to be placed for the desired energy input. One condenser {1a} is a place for the condensation of vapours from the boiling liquids, and second condenser {1b} is placed in chiller unit for cooling of water in the tank. The various instruments will be required in the investigation for the measurement of vacuum in the vessel, the wall and liquid temperatures, and electric energy to the electric heater of the tube. A vacuum/pressure gauge {11} is mount on the top of the test vessel measures the vacuum/pressure in the vessel. The wall and liquid temperature are measured by the copper-constantan thermocouple.

3.2 **Test Surface**

So far it has been discussed and made very clear that the modifications on the surface are proved to be very effective in passively enhancing the heat transfer performance. Taking this into consideration micro-channel groove enhancement technique was employed for the present study. The required channel geometry was obtained after machining of the plain test section geometry. For the present work, two major test sections were designed. These test sections were fabricated by varying the orientation of the channel grooves and dimensions of the geometric parameters. The channels were generated by using V-groove cross-section geometries over the

test section surface and these channel grooves were orientated circumferentially. The dimensions of the channel geometric parameters were adjusted to generate the two enhanced circumferential V-groove Micro-channel test sections.

Fig 3.2: Photograph of experimental setup

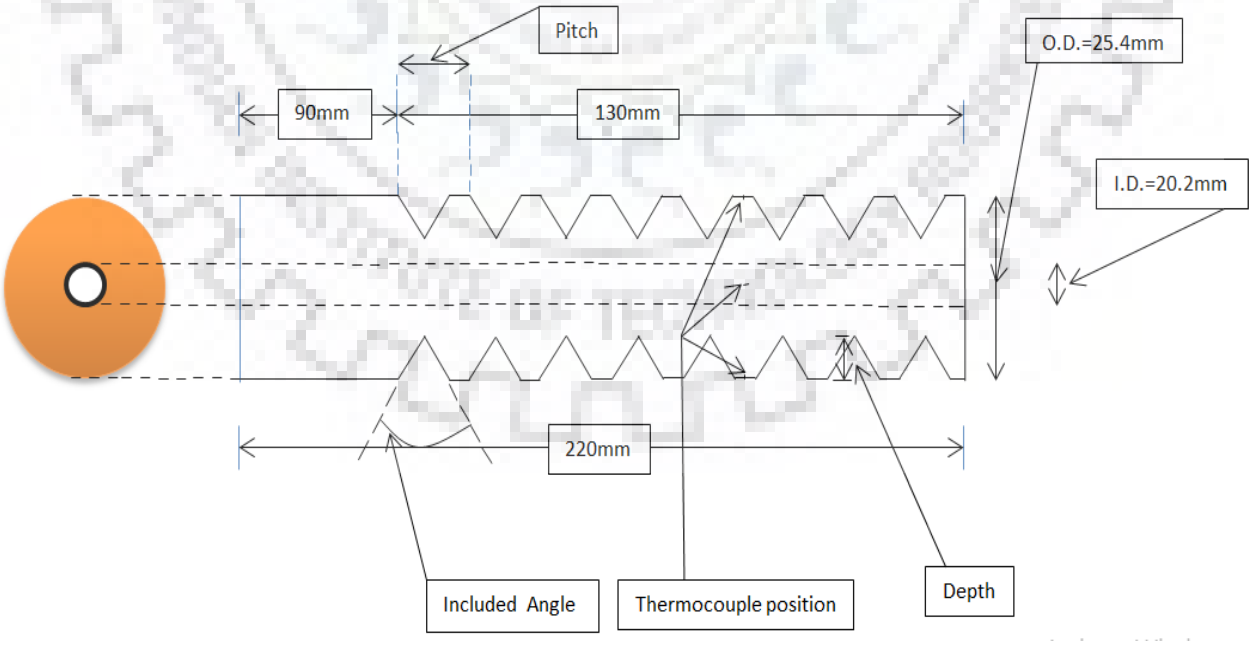

Fig. 3.3: Test Section Geometry

Table 3.1: Dimension details of geometric parameters for micro-finned test section

S. No.	Depth (mm)	Pitch (mm)	Included Angle
1.	1.5	2	60^0
2.	1.5	1.5	45^0

3.3 Refrigerants

In a refrigeration system, the optimum design of the evaporator depends on the right evaluation of the nucleate boiling heat transfer of the refrigerant. In recent years, environmental issues over the use of chlorofluorocarbons have led to the development of different fluids to replace CFC refrigerants. Flooded evaporators are commonly utilized in the heating, ventilating, and air-conditioning (HVAC) trade where the fluid boils outside the tube. These applicates are mainly commercial and industrial based.

For the present study, the following refrigerants are used in the experimental set-up and results have been processed further:

R-134a (1, 1, 1, 2-Tetrafluoroethane)

- ODP-0, GWP-1300
- Used as a substitute for R12 and to a limited range for R22
- Good performance in medium and high temperature application
- Toxicity is very low
- Not miscible with mineral oil

R-404a (azeotropic blend of HFC refrigerants R-125, R-143a, and R-134a)

- ODP- 0, GWP- 3943
- Used as replacement for ozone depleting refrigerants R-502 and R-22 in new and existing equipment
- Good performance in Medium and low temperature application
- No rapid reaction with air and water

- Compatible with polyolester lubricant

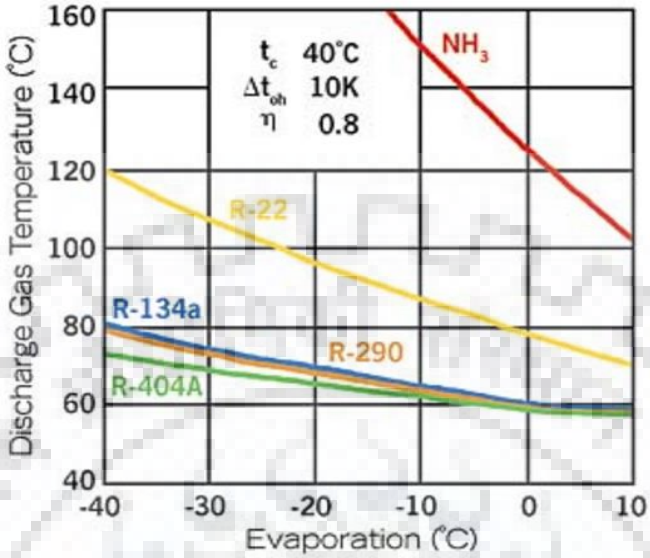

Figure 3.3: Comparison of various discharge gas temperatures. *(Courtesy of Bitzer International.)*

It was noted that propane's pressure levels and the refrigeration capacity are like R-22 and R-502, and its temperature behaviour in CFC system can be used here as a lubricant over a wide application range. Industries have been using refrigeration plants with R-290 worldwide for several years and it has been one among the well-tried refrigerants. R-290 is widely used in smaller compact systems with low refrigerant charges, like residential A/C units and heat pumps and hence the applications for the refrigerants are extended to smaller systems efficiently. Further, the applications are also due to commercial refrigeration systems and chillers and the trend have been found to be positive. Other refrigerants used include R-600a (isobutene) or R-170 (ethane) and they also offer the similar results. Similar results for good performance are expected with halocarbon refrigerants as favourable as R-12 and R-502.

CHAPTER 4

4 Experimental Procedure

The experimental procedure for R-134a and R-404a are as follows:

1. The boiling vessel and test tube were initially cleaned and leak checked before it was evacuated and ensured the non-availability of non-condensable gases in the vessel.
2. The system was charged with the refrigerants up to 20 mm higher than the top of the test tube.
3. To maintain the constant system pressure, the mass flow rate of the condenser liquid was adjusted for each power input and the experiments were performed for refrigerants R-134a and R-404a at saturation temperatures of 21^{o}C.
4. Before running each test, the refrigerants were gradually preheated using an auxiliary heater and their temperatures were compared to the corresponding its saturated state.
5. The data were taken under the steady state conditions as given saturation temperatures from 5 to 40 kW/m^2 with an interval of 5 kW/m^2 and also taken in the order of decreasing heat flux to avoid a hysteresis effect.
6. All the data signals are converted and compiled by an Adam 4019 module. The refrigerant was changed and the same steps (1to5) repeated after the heat transfer surface was cleaned.

Data Reduction and Experimental Results

The nucleate boiling heat transfer coefficient for each power input was determined by equation (4.1):

$$h = \frac{q}{T_w - T_{sat}} \tag{4.1}$$

Where q, T_w, T_{sat} are the power input to the cartridge heater per unit surface area of the tube, arithmetic mean of wall temperature and saturation temperature respectively. In this experiment, nucleate pool boiling heat transfer measurements were performed with R-134a and R-404a refrigerants at 21^{o}C saturation temperatures. Measured heat transfer coefficient of R-134a and R-404a were compared with correlations by Stephan and Abdelsalam's [22], Jung [21] , Cooper[24, 25, 26] and by Gorenflo[23], which is

Given as:

1) Stephan and Abdelsalam correlation [22]

Stephan and Abdelsalam correlation [22] derived from a regression analysis of many data is expressed as follows:

$$h = 207 \frac{k_l}{d}\left(\frac{qd}{k_l T_{sat}}\right)^{0.745}\left(\frac{\rho_v}{\rho_l}\right)^{0.581}(pr_l)^{0.533} \quad (4.2)$$

$$d = 0.0146\emptyset\sqrt{2\sigma/g(\rho_l - \rho_v)} \quad (4.3)$$

Where $\emptyset = 35^{o}$

h is expressed in W/m^2K, q in W/m^2 and pr is the prandtl number.

2) Cooper correlation [24, 25]

The expression of the Cooper correlation [24, 25] is given by following equation:

$$h = 90(p_r)^{(0.12-0.2\log R_p)}(-\log p_r)^{-0.55}(M)^{-0.5}(q)^{0.67} \quad (4.4)$$

where the surface roughnessR_p is taken as 0.4 in the present calculation, *M* is the molar mass expressed in g/mol,and p_r is the reduced pressure that is the ratio between the saturation and critical pressures, depends on the refrigerant properties.

3) Gorenflow correlation[20]

This correlation is based on the reduced pressure and surface roughness. The nucleate boiling heat transfer coefficient at experimental conditions is then calculated relative to the reference heat transfer coefficient using the following equation:

$$h = h_{ref}F_{pf}\left(\frac{q}{q_{ref}}\right)^{n}.\left(\frac{R_p}{r_{p,ref}}\right)^{0.133} \quad (4.5)$$

where pressure correction factor F_{pf} is given as:

$$F_{pf} = 1.2pr^{0.27} + 2.5pr + \frac{pr}{1-pr} \quad (4.6)$$

And exponent:

$$n = 0.9 - 0.3pr^{0.3} \tag{4.7}$$

4) Jung correlation

This correlation is based upon the measured data of eight pure refrigerants following both Stephan-Abdelsalam's and Cooper approaches and also is a strong function of reduced pressure. The Jung correlation is given as:

$$h = 41.4 \frac{K_l}{d}\left[\frac{q\,d}{K_l\,T_{sat}}\right]^c (-\log_{10} pr)^{-1.52}\left(\frac{\rho_l-\rho_v}{\rho_l}\right)^{0.53} \tag{4.8}$$

$$c = 0.835(1-pr)^{1.33} \tag{4.9}$$

The heat transfer coefficient as a function of the heat flux for the plain tube and estimated using the above correlations are plotted for the 21^0 saturation temperatures in Fig 4.1 and Fig 4.2. In this experiment, nucleate pool boiling heat transfer coefficient measurements over a plain tube were carried out with pure fluid (R-134a) and azeotropic fluid (R-404a) at various saturation temperatures. Table 4.1 lists some properties of these refrigerants calculated by REFPROP program [26].

Table 4.1. Properties of tested refrigerants at 21°C [26]

Refrig-erant	T_{sat}	P_{sat}	p_r	T_r	μ x 10^{-4}	K_l	ρ_l	ρ_v	σ x 10^{-3}	M	C_p
	^{0}C	kPa			Pa.s	m^2/s	Kg/m^3	Kg/m^3	N/m	g/mol	KJ/kg K
R-134a	21	590.16	0.1453	0.7857	2.208	0.0778	1220.7	28.659	8.7012	102.03	0.8252
R-404a	21	1127.9	0.302	0.851	1.63	0.0647	1067.2	56.93	4.938	97.6	1.53

4.1 **Experimental results for plain tube**

Fig. 4.1 and Fig. 4.2 show the comparison of heat transfer coefficient vs heat flux for both refrigerants between the present experimental data and correlations. These figures show that HTCs increases confirming the pool boiling theory that the minimum superheat required to activate given cavity sizes as the heat flux increases. The heat transfer coefficient as a function of the heat flux on plain tube and estimated using the above correlations are shown for the saturation temperature in Fig 4.1 and Fig 4.2. For 21^{o}C the Jung [21] and Gorenflo [23] correlations provide better fit of the present experimental data and Jung correlation [21] also gives a good estimate for R-404a. A slight under and over-predictions of the cooper [24, 25] and Gorenflo [23] correlations is observed for a heat flux over 20 kW/m^2. For comparison purpose, the various researcher's correlations are also drawn in the figure. As seen, Stephan and Abdelsalam [22] correlation considerably over predicted the experimental data for R-134a and R-404a at saturation temperature 21^{o}C. Generally, for R-134a, about 20-25% over predictions for the Stephan and Abdelsalam [22] correlation are reported at 21^{o}C saturation temperature.

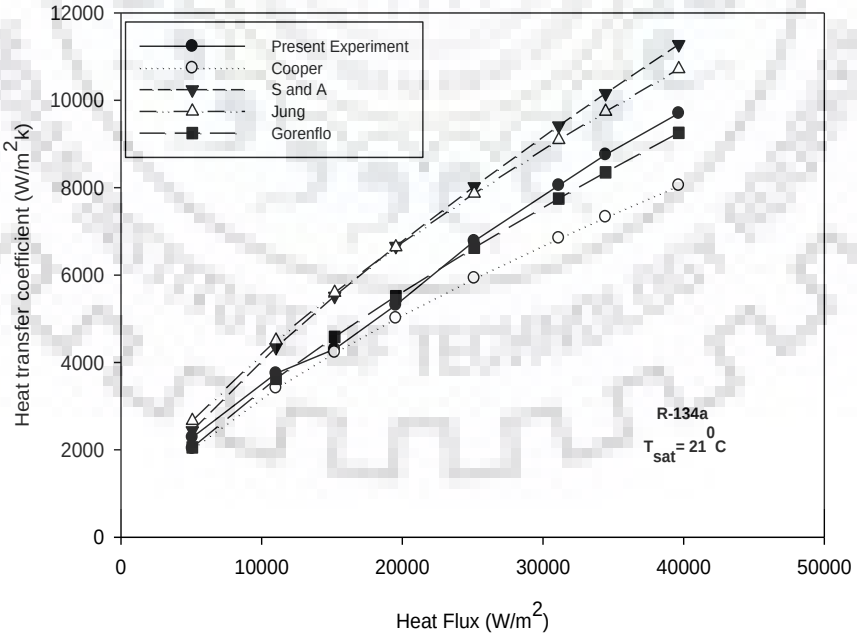

Fig 4.1. Comparison of the present data for R-134a with correlations

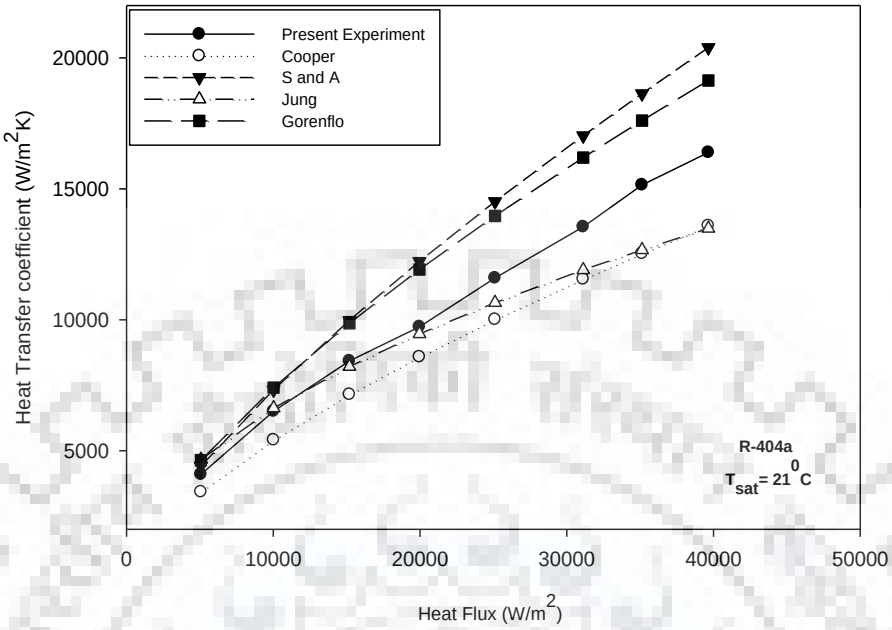

Fig 4.2. Comparison of the present data for R-404a with correlations

The prediction accuracy of the correlations was assessed and compared. The results of this comparison at 21^{o}C saturation temperatures for R134a and R-404a are presented in table 4.2. The prediction mean error was calculated using the following equation:

$$Mean\ error = \frac{1}{n}\sum_{i=1}^{n}\left(\frac{h_{Pred}-h_{Exp}}{h_{Exp}}\right)_i \qquad (5)$$

It can be clearly seen in the table 4.2 that the Gorenflo [23] correlation provides good agreement of the experimental data with a maximum mean error of -2% for R-134 and -5% for R-404a at given saturation temperature conditions. The Cooper [24, 25] correlation under-predicts both refrigerants with a maximum mean error of -15%. Fig 4.4 indicates the boiling curve for the plain tube for both refrigerants at saturation temperature of 21^{o}C.

Table 4.2. Accuracy of various correlations at 21^0C

Refrigerant	**Correlations**	**Experimental Condition**	**Mean error [%]**
			21^oC
R-134a	Stephan-Abdelsalam [22]	q=5 to 40 kW/m^2 no of data points=8	17.96
	Cooper [24,25]		-11.025
	Jung [21]		17.79
	Gorenflo [23]		-2.3
R-404a	Stephan-Abdelsalam[22]		20.322
	Cooper [24,25]		-15.358
	Jung [21]		-5.513
	Gorenflo [23]		17.437

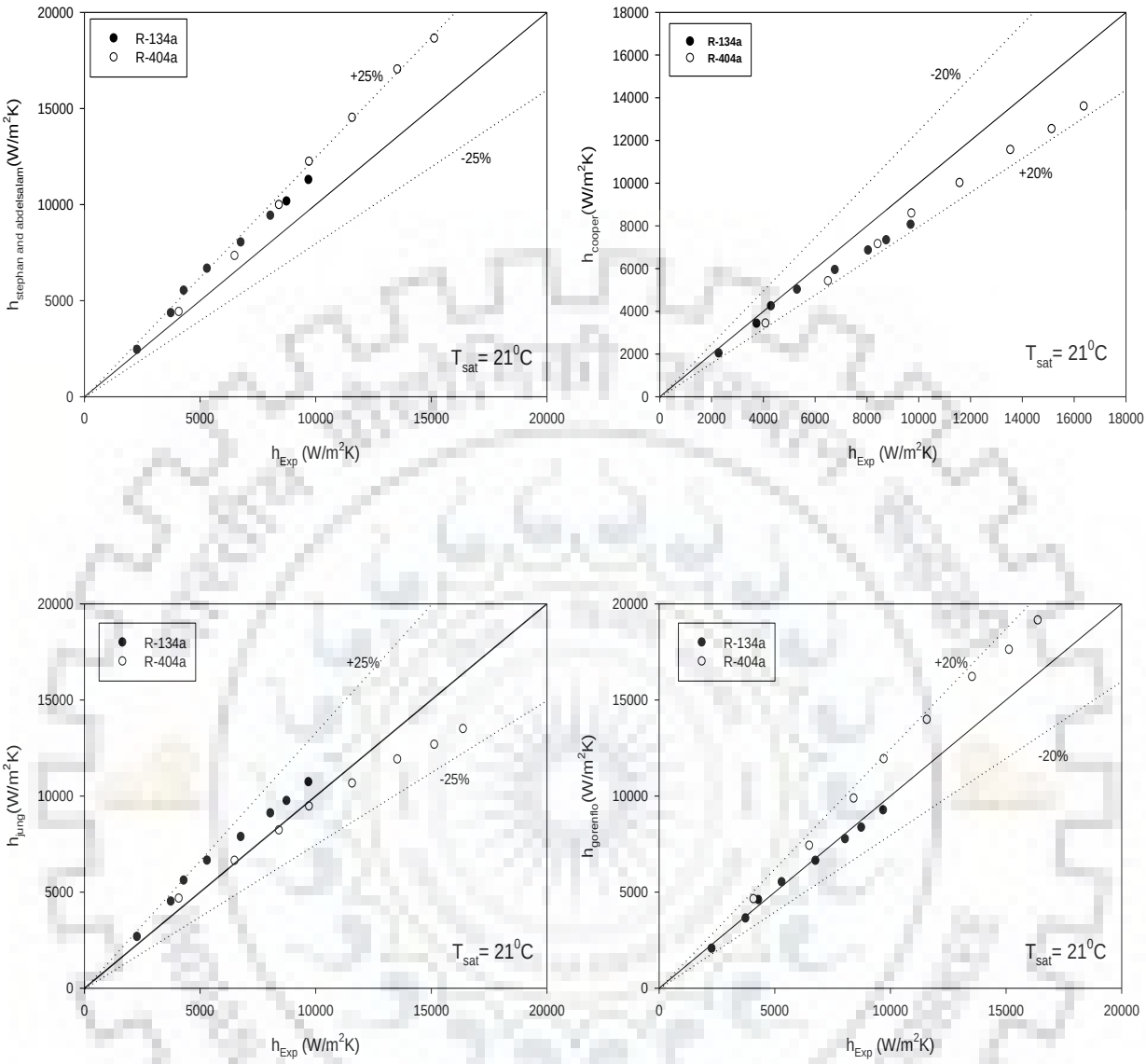

Fig 4.3: Error percentage of correlations with experimental data

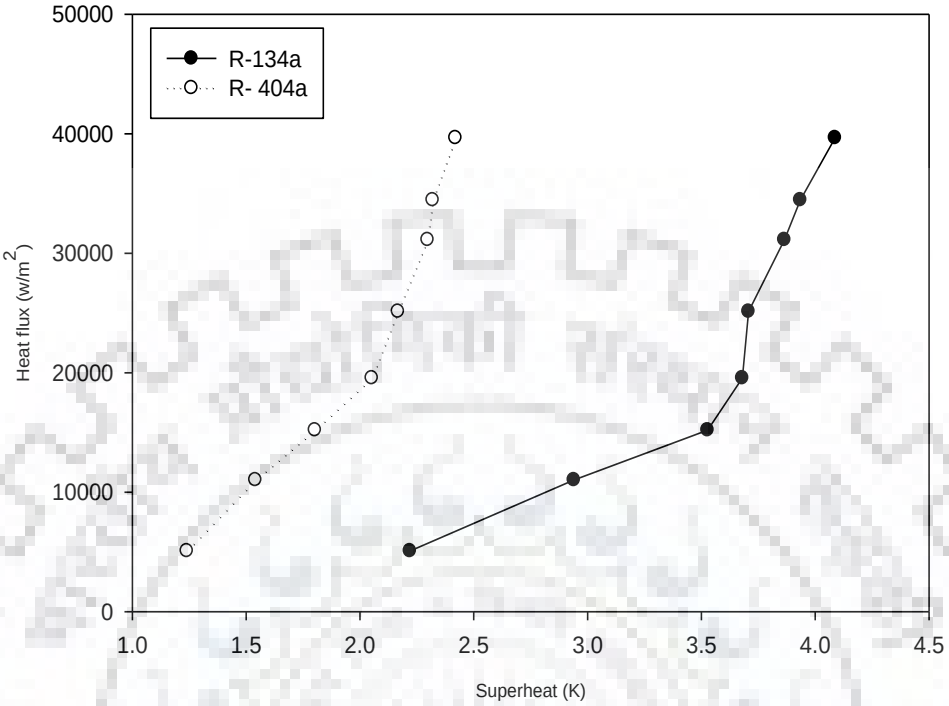

Fig 4.4: Boiling curve for the plain tube (heat flux vs superheat).

The required amount of superheat increases by increasing the saturation temperatures with the condition of lower heat flux (<40kW/m^2) in the case of a plain tube. This criteria arises probably due to lower activation of nucleation sites. In general, Cooper [25, 26] and Jung [21] correlations under predicted the HTCs of pure and quasi-refrigerants. Jung [21] correlation under predicted the HTCs of refrigerants at all saturation temperatures showing an average deviation lies between 5 to 20% for R-134a and -10 to 5% for R-404a. Alternatively, Cooper correlation shows -17 to -10% for R-134a and -20 to -5% for R-404a. It under predicted the HTCs of R-134a and R-404a in the range of 45 to 72%. Stephan and Abdelsalam's [22] correlation over predicted the HTCs of refrigerants by 17% due to the database were not consistent during the development of correlation. As shown in Fig.5, Gorenflo [23] and Jung-[21] correlations were well balanced for both refrigerants at saturation temperature of 21^{o}C and also Gorenflo [23] correlation over predicted the data by 20%.

Experimental data for Plain and Finned surface Tube:

Table 4.3 Plain tube in R-134a refrigerant

Voltage (V)	Current (I)	Surface area (m^2)	Heat flux (q) (W/m^2)	Wall Surface Temperature (K)				Average wall temperature	Liquid Temp. (T_l)	Wall superheat (T_w-T_l)	Heat transfer coefficient (h)
				T_t	T_b	T_{s1}	T_{s2}				
54	0.87	9.256	5075.626621	22.65	21.93	22.1	22.2	22.22	20	2.22	2286.318298
81	1.26	9.256	11026.36128	25.56	23.98	24.31	24.35	24.55	21.61	2.94	3750.46302
95	1.48	9.256	15190.14693	25.26	23.72	24.5	24.55	24.5075	20.98	3.5275	4306.207493
109	1.66	9.256	19548.40104	25.16	24.11	24.9	24.95	24.78	21.1	3.68	5312.065499
125	1.86	9.256	25118.84183	24.99	23.9	24.48	24.54	24.4775	20.77	3.7075	6775.142773
134	2.15	9.256	31125.75627	25.09	23.91	24.3	24.32	24.405	20.54	3.865	8053.235774
143	2.23	9.256	34452.24719	25.39	23.97	24.44	24.54	24.585	20.65	3.935	8755.336008
148	2.48	9.256	39654.27831	25.43	23.91	24.44	24.57	24.5875	20.5	4.0875	9701.352491

Table 4.4 Plain tube in R-404a refrigerant

Voltage (V)	Current (I)	Surface area (m^2)	Heat flux (q) (W/m^2)	Wall Surface Temperature (K)				Average wall temperature (T_w)	Liquid Temp. (T_l)	Wall superheat (T_w-T_l)	Heat transfer coefficient (h)
				T_t	T_b	T_{s1}	T_{s2}				
54	0.87	9.256	5075.626621	22.82	21.49	21.63	21.62	21.89	20.65	1.24	4093.247275
81	1.26	9.256	11026.36128	23.52	21.55	22.13	22.16	22.34	20.799	1.541	6507.521017
95	1.48	9.256	15190.14693	23.62	21.73	22.31	22.23	22.4725	20.67	1.8025	8427.265982
109	1.66	9.256	19548.40104	23.88	22	22.81	22.84	22.8825	20.83	2.0525	9727.370441
125	1.86	9.256	25118.84183	23.98	22.14	22.95	22.96	23.0075	20.84	2.1675	11588.85436
134	2.15	9.256	31125.75627	24.77	22.8	24.23	24.23	24.0075	21.71	2.2975	13547.66323
143	2.23	9.256	34452.24719	24.8	22.3	23.74	23.72	23.64	21.32	2.32	15143.02
148	2.48	9.256	39654.27831	24.98	23.11	23.87	23.88	23.96	21.54	2.42	16386.06542

Table 4.5 Finned tube with 45^0 included angle in R-134a refrigerant

Voltage (V)	Current (I)	Surface area (m^2)	Heat flux (q) (W/m^2)	Wall Surface Temperature (K)				Average wall temperature (T_w)	Liquid Temp. (T_l)	Wall superheat (T_w-T_l)	Heat transfer coefficient (h)	Enhancement factor over plain tube
				T_t	T_b	T_{s1}	T_{s2}					
75	1.11	16.976	4903.982092	22.65	21.93	22.1	22.2	22.22	20.87	1.35	3632.579328	1.588832
106	1.6	16.976	9990.574929	23.8	23.1	23.24	23.26	23.35	21.56	1.79	5581.326776	1.488171
129	1.97	16.976	14969.95759	24	23.71	23.89	23.87	23.8675	21.47	2.3975	6243.986481	1.449999
143	2.37	16.976	19964.06692	24.45	23.9	24.1	24.13	24.145	21.56	2.585	7723.043295	1.45387
162	2.61	16.976	24906.92743	24.51	23.99	24.13	24.21	24.21	21.59	2.62	9506.46085	1.403139
176	2.89	16.976	29962.29972	24.63	23.99	24.19	24.15	24.24	21.49	2.75	10895.38172	1.352921
191	3.1	16.976	34878.65221	24.79	23.97	24.23	24.23	24.305	21.35	2.955	11803.2664	1.348124
208	3.3	16.976	40433.55325	24.9	24.23	24.44	24.43	24.5	21.34	3.16	12795.42824	1.318933

Table 4.6 Finned tube with 60^0 included angle in R-134a refrigerant

Voltage (V)	Current (I)	Surface area (m^2)	Heat flux (q) (W/m^2)	Wall Surface Temperature (K)				Average wall temperature (T_w)	Liquid Temp. (T_l)	Wall superheat (T_w-T_l)	Heat transfer coefficient (h)	Enhancement factor over plain tube
				T_t	T_b	T_{s1}	T_{s2}					
68	1.05	14.173	5037.74783	22.87	22.3	22.61	22.62	22.6	21.2	1.4	3598.391307	1.573879119
99	1.43	14.173	9988.710929	23.68	23.23	23.45	23.46	23.455	21.54	1.915	5216.037039	1.390772609
119	1.8	14.173	15113.24349	23.94	23.64	23.87	23.88	23.8325	21.32	2.5125	6015.22129	1.396874574
132	2.13	14.173	19837.71961	24.34	23.89	24.21	24.25	24.1725	21.54	2.6325	7535.695957	1.418601438
146	2.45	14.173	25238.12884	24.48	23.98	24.14	24.14	24.185	21.47	2.715	9295.811726	1.372047179
162	2.61	14.173	29832.78064	24.62	24	24.1	24.12	24.21	21.38	2.83	10541.6186	1.308992615
172	2.88	14.173	34950.9631	24.76	24.1	24.21	24.13	24.3	21.23	3.07	11384.67853	1.300314041
187	3.05	14.173	40242.00945	24.9	24.24	24.32	24.32	24.445	21.24	3.205	12556.00919	1.294253809

Table 4.7 Finned tube with 45^0 included angle in R-404a refrigerant

Voltage (V)	Current (I)	Surface area (m^2)	Heat flux (q) (W/m^2)	Wall Surface Temperature (K)				Average wall temperature (T_w)	Liquid Temp. (T_l)	Wall superheat (T_w-T_l)	Heat transfer coefficient (h)	Enhancement factor over plain tube
				T_t	T_b	T_{s1}	T_{s2}					
76	1.11	16.976	4969.36852	22.41	22.12	22.32	22.31	22.29	21.49	0.8	6211.71065	1.517553491
106	1.6	16.976	9990.574929	22.57	22.23	22.42	22.43	22.4125	21.38	1.0325	9676.101626	1.486910778
129	1.97	16.976	14969.95759	22.68	22.35	22.54	22.55	22.53	21.21	1.32	11340.87696	1.345737162
143	2.37	16.976	19964.06692	22.87	22.4	22.62	22.68	22.6425	21.12	1.5225	13112.68763	1.348019828
162	2.66	16.976	25384.07163	23.1	22.81	22.9	22.94	22.9375	21.24	1.6975	14953.79772	1.290360797
176	2.89	16.976	29962.29972	23.34	22.9	23.12	23.14	23.125	21.44	1.685	17781.78025	1.312535172
191	3.14	16.976	35328.69934	23.49	23.21	23.32	23.32	23.335	21.53	1.805	19572.68662	1.292522008
208	3.3	16.976	40433.55325	23.53	23.31	23.47	23.47	23.445	21.42	2.025	19967.18679	1.218547155

Table 4.8 Finned tube with 60^0 included angle in R-404a refrigerant

Voltage (V)	Current (I)	Surface area (m^2)	Heat flux (q) (W/m^2)	Wall Surface Temperature (K)				Average wall temperature (T_w)	Liquid Temp. (T_l)	Wall superheat (T_w-T_l)	Heat transfer coefficient (h)	Enhancement factor over plain tube
				T_t	T_b	T_{s1}	T_{s2}					
68	1.05	14.173	5037.74783	22.43	22.12	22.24	22.23	22.255	21.39	0.865	5823.985931	1.422830308
99	1.43	14.173	9988.710929	22.57	22.25	22.38	22.37	22.3925	21.32	1.0725	9313.483384	1.431187823
119	1.8	14.173	15113.24349	22.68	22.31	22.56	22.53	22.52	21.12	1.4	10795.17392	1.280982659
132	2.13	14.173	19837.71961	22.86	22.41	22.58	22.57	22.605	21	1.605	12359.94991	1.27063635
146	2.45	14.173	25238.12884	23.12	22.82	22.98	22.97	22.9725	21.23	1.7425	14483.8616	1.249810085
162	2.61	14.173	29832.78064	23.34	22.91	23.21	23.2	23.165	21.38	1.785	16713.04237	1.233647905
172	2.88	14.173	34950.9631	23.48	23.22	23.34	23.34	23.345	21.48	1.865	18740.46279	1.237564422
187	3.05	14.173	40242.00945	23.52	23.34	23.48	23.47	23.4525	21.39	2.0625	19511.27731	1.190724147

4.2 **Experimental results for finned surface**

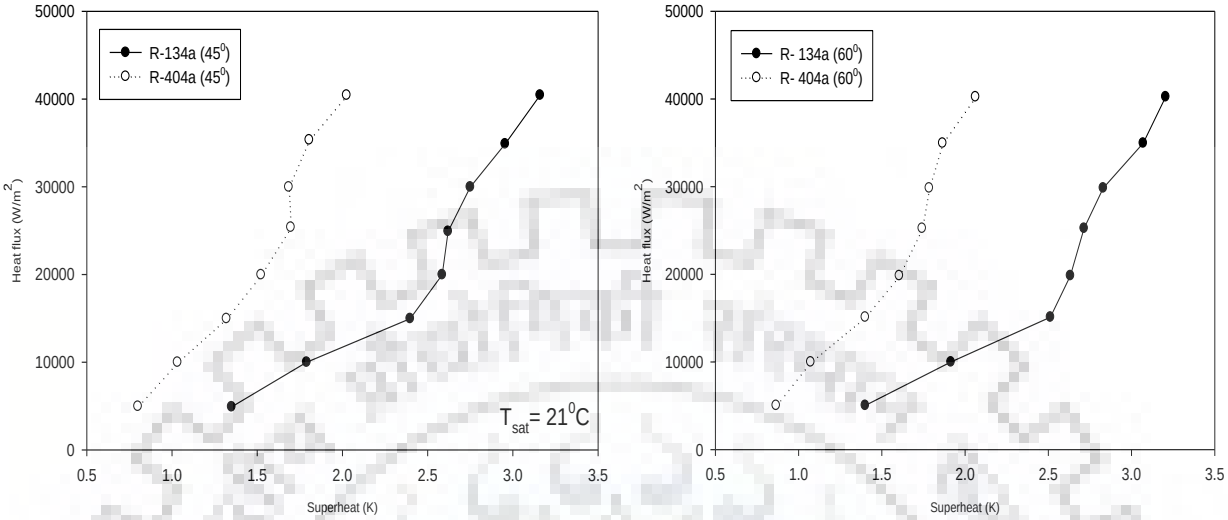

Fig 4.5: Comparison of Boiling curve between refrigerants R134a and R404a

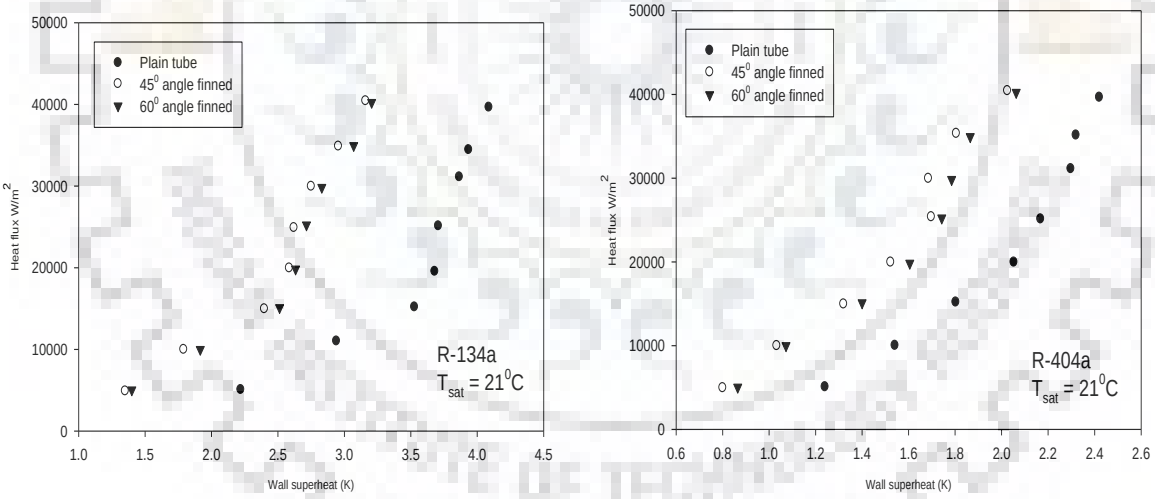

Fig 4.6: Comparison boiling curve of Plain tube over finned surface tube

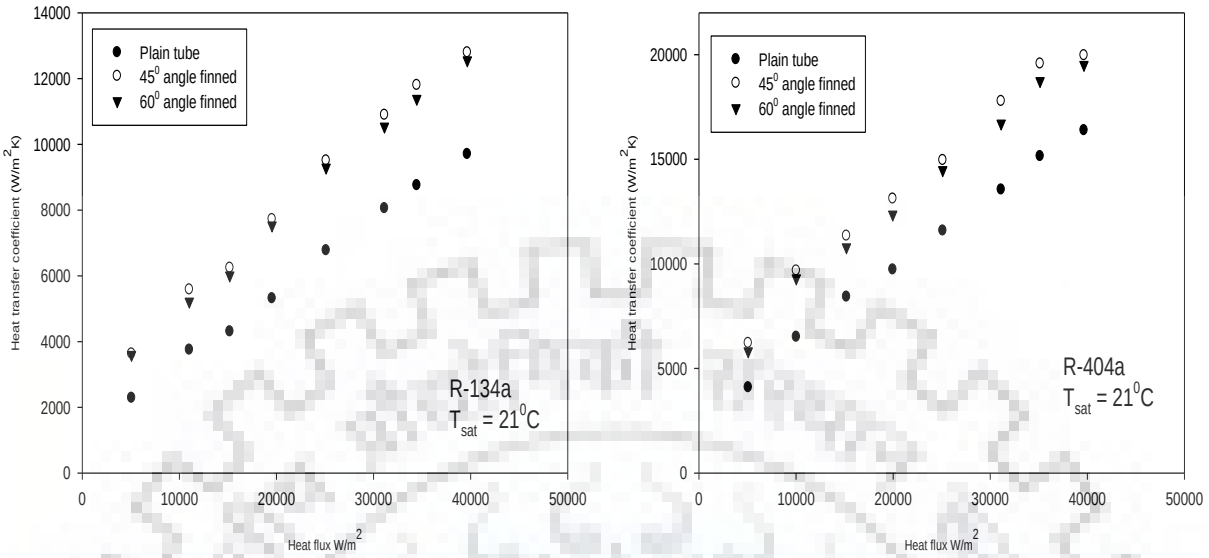

Fig 4.7: Comparison of Heat transfer coefficients

For the evaluation and validation of current data of resultant radial heat flux, the wall superheat, and the heat transfer coefficient under different testing conditions, earlier proposed data reduction equations were used. After applying data reduction equations, the resultant reduced data was used to plot the performance curves for the plain surface and the finned test sections. The boiling curves generated for the test sections in the horizontal orientation using present experimental data show significant performance enhancements with channel surfaces compared to a plain surface and are shown in Fig. 4.7. The plain test section was tested for a maximum heat flux of approximately 40kW/m^2 and the finned test sections were tested up to a heat flux of exactly 40kW/m^2 successfully. In plain test section, wall superheat of almost 4.2 K for R-134a and 2.42 K for R-404a refrigerant was recorded yielding boiling heat transfer coefficient of 9.7kW/m^2 K for R-134a and 16kW/m^2 for R-404a. A minimum wall superheat of 0.8 K was observed with test section 45^0 angle groove in R-404a and slight higher 1.35K in R-134a refrigerant at same finned surface at mentioned heat flux conditions.

CHAPTER 5

5 Conclusions and Future Scope

The nucleate pool boiling of R-134a and R-404a was investigated on plain and finned copper tubes through experiments performed at saturation temperature of 21^0C and heat fluxes from 5 and 40kW/m^2 in the interval of 5.

From literature it is clear that, for a given heat flux, the boiling heat transfer coefficient increases with an increase in saturation temperature for a plain tube. The heat transfer coefficient for R-134a is lower as compared to R-404a at given saturation temperature due to its lower reduced pressure. It is also shown that Jung [21], Gorenflo [23] and Cooper [24, 25] correlations predicts the present experimental data satisfactorily.

The heat transfer coefficient is higher for the finned tube than for the plain tube of about the factor range between 1.2- 1.6 for in R-404a and 1.1- 1.5 for R-134a. This enhancement of the heat transfer due to the fins is high at low heat flux and with the increase of heat flux, enhancement of heat transfer coefficient decreases gradually. This phenomenon is proposed to be caused by the large bubbles growing on the tube surface which decreases heat transfer coefficient. While on the plain tube, a dried area appears at the foot of the bubbles and on the finned tube some liquid is trapped in the fins enabling a stronger heat transfer at the bubble foot.

References

[1] Faghri, A., Zhang, Y. and Howell, J.R., "*Advanced heat and mass transfer".* 2010 Global Digital Press.

[2] Bejan, A. and Kraus, A.D., "*Heat transfer handbook"* (Vol. 1). 2003 John Wiley & Sons.

[3] Henrick Gjerkes, Imk Golobic "Measurement of certain parameters influencing the activity of nucleation sites in Pool boiling" Experimental Thermal and Fluid science 2002. pp487-493

[4] Hahne, E., Chen, Q., Windisch, R., Pool boiling heat transfer on finned tubes: an experimental and theoretical study. Int. J. Heat Mass Transfer 34 (8) 1991., 2071-2079.

[5] Park, K.-J., and Jung, D., "Nucleate Boiling Heat Transfer Coefficients of R1234yf on Plain and Low Fin Surfaces," Int. J. Refrigeration, 33(3) 2010. pp. 553–557.

[6] Forrest, E. C., Hu, L.-W., Mckrell, T. J., Buongiorno, J., and Ostrovsky, Y., "Pressure Effects on the Pool Boiling of the Fluorinated Ketone C2F5C(O)CF(CF3)2," Proc. ITherm 2010, Las Vegas, NV.

[7] Se´rgio Pereira Rocha, Olivier Kannengieser, Elaine Maria Cardoso, Ju´ lio Ce´sar Passos, refrigeration 36 , 2013 pp. 456-464

[8] Hsieh, S.S. , Yang, T.Y. , Nucleate pool boiling from coated and spirally wrapped tubes in saturated R-134a and R-600a at low and moderate heat flux, Trans. ASME J. Heat Transfer 123 (2) 2001, pp.257–270.

[9] Ribatski, G. , Saiz Jabardo, J.M., Experimental study of nucleate boiling of halocarbon refrigerants on cylindrical surfaces, Int. J. Heat Mass Transfer 46 (23) , 2003. 4439–4451.

[10] Kang, M.G., Effects of tube inclination on pool boiling heat transfer, Nucl. Eng. Des. 220 (1), 2003, pp. 67–81.

[11] Chien, L.H., Webb, R.L., A parametric study of nucleate boiling on structured surfaces. I. Effect of tunnel dimensions, Trans. ASME J. Heat Transfer 120 (4) , 1998, pp. 1042–1048.

[12] Thome, J. R., "Mechanisms of Enhanced Nucleate Pool Boiling," Proceedings of the Engineering Foundation Conference on Pool and External Flow Boiling, ASME, New York, 1992, pp. 337-343

[13] Hsieh, S.S. , Yang, T.Y. , Nucleate pool boiling from coated and spirally wrapped tubes in saturated R-134a and R-600a at low and moderate heat flux, Trans. ASME J. Heat Transfer 123 (2) , 2001, pp.257–270.

[14] Cieslinski, J.T., Nucleate pool boiling on porous metallic coatings, Exp. Thermal Fluid Sci. 25 (7), 2002, pp.557–564.

[15] Kim, J.H. , Rainey, K.N. , You, S.M. , Pak, J.Y. , Mechanism of nucleate boiling heat transfer enhancement from microporous surfaces in saturated FC-72, Trans. ASME J. Heat Transfer 124 (3), 2002,pp. 500–506.

[16] Webb,R.L., Pais, C.,Nucleate pool boiling data for five refrigerants on plain, integral-fin and enhanced tube geometries, Int. J. Heat Mass Transfer 35 (8), 1992, pp.1893–1904.

[17] Memory, S.B., Sugiyama, D.C. P.J. Marto, D.C., Nucleate pool boiling of R-114 and R-114-oil mixtures from smooth and enhanced surfaces. I. Single tubes, Int. J. Heat Mass Transfer 38 (8), 1995, pp.1347–1361.

[18] Rajulu, K.G., Kumar, Mohanty, B, Varma, H.K. Enhancement of nucleate pool boiling heat transfer coefficient by reentrant cavity surfaces, Heat and Mass Transfer/Waerme-und Stoffuebertragung 41 (2), 2004, pp.127–132

[19] G. Ribatski, J.R. Thome, Nucleate boiling heat transfer of R134a on enhanced tubes, Appl. Therm. Eng. 26 (10), 2006, pp.1018–1031.

[20] Chien, L.H., Webb, R.L., Visualization of pool boiling on enhanced surfaces, Exp. Thermal Fluid Sci. 16 (4) , 1998. pp. 332–341.

[21] Nakayama, T., Daikoku, Kuwahara, H., Nakajima, T. , Dynamic model of enhanced boiling heat transfer on porous surfaces. I. An experimental investigation, Trans. ASME J. Heat Transfer 102 (3), 1980, pp. 445–450.

[22] Cooke, D., Kandlikar, S.G., Pool boiling heat transfer and bubble dynamics over plain and enhanced microchannels, J. Heat Transfer 133 (5), 2011.

[23] Jung D., et al., Nucleate Boiling Heat Transfer Coefficients of Pure Halogenated Refrigerants, Int. J. Refrigeration, 26, 2, (2003) 240-248.

[24] Stephan, K., Abdelsalam, K., Heat transfer correlation for natural convection boiling, International Journal of Heat and Mass Transfer, Vol.23, 1980, pp. 73-87.

[25] Gorenflo, D., Pool boiling, VDI Heat Atlas, (chapter Ha), 1993

[26] Cooper, M.G., Saturation Nucleate Pool Boiling a Simple Correlation, IChemE Symposium, Series 86, (1984)786-793.

[27] Cooper, M.G., Heat flow rates in saturated nucleate pool boiling-a wide-ranging examination using reduced properties, Advances in Heat Transfer, 16, (1984) 157-239.